AD-A068 388 AERONAUTICAL RESEARCH ASSOCIATES OF PRINCETON INC N J F/G 20/4
EVALUATION OF TURBULENCE MODELS FOR ROCKET AND AIRCRAFT PLUME F--ETC(U)
FEB 79 H S PERGAMENT, S M DASH, A K VARMA N00123-78-C-0010
UNCLASSIFIED ARAP-370-VOL-1 NL

| OF |
AD
A068388

END
DATE
FILMED
6-79
DDC

A.R.A.P. Report No. 370-I

LEVEL

EVALUATION OF TURBULENCE MODELS FOR ROCKET AND AIRCRAFT PLUME FLOWFIELD PREDICTIONS

H.S. Pergament
S.M. Dash
A.K. Varma

Aeronautical Research Associates of Princeton, Inc.
50 Washington Road, P.O. Box 2229
Princeton, New Jersey 08540

Final Report, Vol. I

February 1979

Prepared For
NAVAL WEAPONS CENTER
China Lake, California 93555
Contract N00123-78-C-0010

Unclassified

SECURITY CLASSIFICATION OF THIS PAGE (When Data Entered)

(9) Final rept.

REPORT DOCUMENTATION PAGE

READ INSTRUCTIONS BEFORE COMPLETING FORM

1. REPORT NUMBER: Report # 370-I
2. GOVT ACCESSION NO.:
3. RECIPIENT'S CATALOG NUMBER:

4. TITLE (and Subtitle): (6) Evaluation of Turbulence Models for Rocket and Aircraft Plume Flowfield Predictions. Volume I.
5. TYPE OF REPORT & PERIOD COVERED: Technical Report
6. PERFORMING ORG. REPORT NUMBER: Report # 370-I

7. AUTHOR(s): (10) H. S. Pergament, S. M. Dash, A. K. Varma
8. CONTRACT OR GRANT NUMBER(s): (15) N00123-78-C-0010

9. PERFORMING ORGANIZATION NAME AND ADDRESS:
ARAP
50 Washington Road, P.O. Box 2229
Princeton, NJ 08540

10. PROGRAM ELEMENT, PROJECT, TASK AREA & WORK UNIT NUMBERS:
Program Element 62332N
Proj: ZF32-392-002
RDT&E AD1791319

11. CONTROLLING OFFICE NAME AND ADDRESS:
Commander, Code 39403
Naval Weapons Center
China Lake, CA 93555

(11)

12. REPORT DATE: Feb[redacted]79
13. NUMBER OF PAGES: 42

14. MONITORING AGENCY NAME & ADDRESS (if different from Controlling Office): (12) 47p.

15. SECURITY CLASS. (of this report): Unclassified
15a. DECLASSIFICATION/DOWNGRADING SCHEDULE:

16. DISTRIBUTION STATEMENT (of this Report):
Approved for Public Release; Distribution Unlimited

(16) F32392 (17) ZF32392002

17. DISTRIBUTION STATEMENT (of the abstract entered in Block 20, if different from Report)

(14) ARAP-370-VOL-I

18. SUPPLEMENTARY NOTES:

19. KEY WORDS (Continue on reverse side if necessary and identify by block number)
Rocket Flowfields
Aircraft Plume Flowfields
Turbulence Models
Flowfield Predictions

20. ABSTRACT (Continue on reverse side if necessary and identify by block number)
A systematic evaluation of several turbulence models for use in aircraft & rocket plume flowfield predictions is presented. Eddy viscosity & two equation (TKE) models presently utilized for plume calculations have been incorporated into a mixing/afterburning code (BOAT) & tested against a wide range of laboratory data. These data include incompressible & compressible free shear layers & jets, H_2/air subsonic and subsonic reacting flows & a liquid propellant rocket plume. The significant differences between rocket/aircraft plume flowfields & the laboratory test conditions used to determine the turbulence model "constants" are discussed.

DD FORM 1 JAN 73 1473 EDITION OF 1 NOV 65 IS OBSOLETE
S/N 0102-014-6601

008 400

SECURITY CLASSIFICATION OF THIS PAGE (When Data Entered)

20. ABSTRACT (Cont'd)

The two-equation (K 2) model, with a suitable correction for compressibility, adequately predicts all the nonreacting shear layer and jet cases and the subsonic H_2/air reacting jet case, but does not fare as well in the supersonic H_2/air reacting jet and liquid propellant plume cases. Suggestions are given for K 2 model improvements to account for the noted inadequacies in compressible, reacting flows, and a recommended method for implementing these model improvements is provided.

A.R.A.P. Report No. 370-I

EVALUATION OF TURBULENCE MODELS FOR ROCKET AND AIRCRAFT PLUME FLOWFIELD PREDICTIONS

H.S. Pergament
S.M. Dash
A.K. Varma

Aeronautical Research Associates of Princeton, Inc.
50 Washington Road, P.O. Box 2229
Princeton, New Jersey 08540

Final Report, Vol. I
February 1979

Prepared For

NAVAL WEAPONS CENTER
China Lake, California 93555
Contract N00123-78-C-0010

TABLE OF CONTENTS

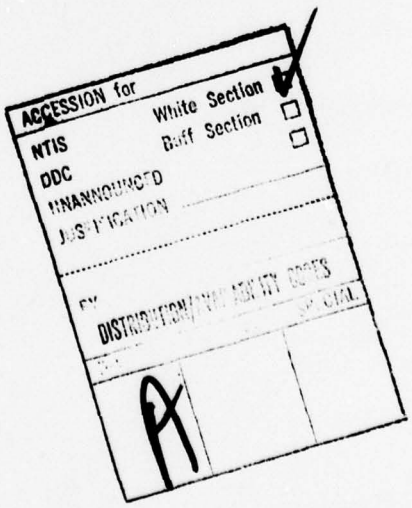

LIST OF FIGURES

LIST OF FIGURES (continued)

EVALUATION OF TURBULENCE MODELS FOR ROCKET AND AIRCRAFT PLUME FLOWFIELD PREDICTIONS

H. S. Pergament, S. M. Dash, and A. K. Varma
Aeronautical Research Associates of Princeton, Inc.
Princeton, New Jersey 08540

Abstract

A systematic evaluation of several turbulence models for use in aircraft and rocket plume flowfield predictions is presented. Eddy viscosity and two equation (TKE) models presently utilized for plume calculations have been incorporated into a mixing/afterburning code (BOAT) and tested against a wide range of laboratory data. These data include incompressible and compressible free shear layers and jets, H_2/air subsonic and supersonic reacting flows and a liquid propellant rocket plume. The significant differences between rocket/aircraft plume flowfields and the laboratory test conditions used to determine the turbulence model "constants" are discussed. It is demonstrated that the eddy viscosity models tested (Donaldson/Gray and extended Prandtl Mixing Length) have an insufficient range of generality for reliable use in flight predictions of aircraft/rocket plumes. The two-equation ($k\varepsilon 2$) model, with a suitable correction for compressibility, adequately predicts all the nonreacting shear layer and jet cases and the subsonic H_2/air reacting jet case, but does not fare as well in the supersonic H_2/air reacting jet and liquid propellant plume cases. Suggestions are given for $k\varepsilon 2$ model improvements to account for the noted inadequacies in compressible, reacting flows. It is emphasized that these improvements must not alter the demonstrated ability of the $k\varepsilon 2$ model to predict the simpler flows. A recommended method for implementing these model improvements is provided. The modified model should provide the basis for more generalized and reliable aircraft/rocket plume predictive capabilities than are presently available.

1. Introduction

The sensitivity of rocket and aircraft plume flowfield predictions to the choice of turbulence model has been well established. Thus, a rational basis for selecting a turbulence model for use in the large computer codes that predict these flowfields has long been a need of the plume community. The validity of a particular turbulence model cannot be established solely on the basis of comparisons between plume model predictions and observable flight data (e.g., IR signatures). Such comparisons involve uncertainties in the overall computational procedure, which includes both flowfield and radiation predictions, as well as atmospheric transmission effects and sensor characteristics. (Dash, et al.[1] specifically address the sensitivity of rocket plume IR signature predictions to flowfield assumptions and turbulence models.) In the present report, we will demonstrate the systematic procedure required to validate proposed turbulence models for use in flight calculations, and arrive at some preliminary recommendations regarding the usefulness of the specific models tested.

Since this is an assessment study, rather than one to develop "new" models, the eddy viscosity and turbulent kinetic energy models chosen for evaluation are those that have been utilized in previous rocket and aircraft plume flowfield studies.

The overriding requirement in this evaluation is that the proposed turbulence model must first be able to predict the large body of well established data on free shear layer and jet flows. These are relatively simple flows (compared to rocket or aircraft plumes), which range in complexity from incompressible two-dimensional shear layers to coaxial reacting H_2/air jets. In addition, since the turbulence models must be placed within a computer code to perform the comparisons with data, a second requirement is that one computer code be used to test all the models. This is essential in order to separate differences in results due to models from differences due to numerical procedures and code structure.

Innumerable studies have been performed in which a specific turbulence model has been tested against a single data set. Far fewer (but still a considerable number of) studies have appeared in the literature in which a specific turbulence model has been compared with a number of data sets. Most noteworthy of the latter are some of the papers presented at the 1972 NASA/Langley Free Turbulent Shear Flows Conference,[2] (e.g., the work of Harsha,[3] Rudy and Bushnell,[4] Peters and Phares,[5] etc.) and the recent work of Evans, et al.[6] Of the studies that have tested a number of turbulence models against a large number of different data sets, the most widely quoted are those of Launder, et al.[7] (in Ref. 2) and Harsha.[8] The models evaluated in the above references have ranged in increasing order of sophistication from simple eddy viscosity models, through one and two equation turbulent kinetic energy models, to models which solve differential equations for the turbulent shear stress.

The approach in the present work is in the same spirit as that of Refs. 7 and 8 with, however, the strong motivation of directing the results of the evaluation toward rocket and aircraft plume calculations. Since these are very complex flowfields (cf., Ref. 9), having conditions widely different from those encompassing the available experimental data base, the maximum amount of generality is required. While this generality is always sought in evaluating turbulence models, the nature of rocket/aircraft plume flowfields is such that for practical applications, the turbulence model will almost always be used for flow situations that are widely different from the conditions under which the models were validated.

In order to implement the above approach, it is necessary to isolate those individual effects which make rocket/aircraft plumes different from the experimental conditions under which the turbulence model "constants" were obtained. In this study, we systematically built up to the complex afterburning rocket plume flows of interest by analyzing successively more complex data sets. Thus, we first return to the simple incompressible flows to validate the turbulence models under conditions where, based on past experience, they should work. We then treat supersonic flows (adding the "compressibility" effect) followed by nonhomogeneous flows (adding the "variable density" effect), subsonic flows with chemistry, supersonic flows with chemistry and finally rocket plumes. None of the cases presented in this study have significant pressure gradient effects. These effects can be important, particularly in highly underexpanded rocket plumes, and will be studied in future efforts.

A recently developed code for treating the turbulent mixing and chemical reactions between coflowing streams is used for this evaluation. The code, named BOAT for its original use in calculating jet entrainment in the vicinity of aircraft nozzle boattails, is described in Refs. 10 and 11. A unique feature for the present evaluation is that the code can either be used in a constant pressure mode, or can be overlaid on a prescribed inviscid flow, which gives inner and outer shear layer edge properties and pressure gradients. The BOAT code is presently being used for rocket and aircraft plume flowfield predictions (e.g., Ref. 1) and will be extensively utilized in the future by a wide segment of government and industry as a "module" within the JANNAF Standard Plume Model (now under development at A.R.A.P. - see Ref. 9). For the purpose of this study, it is a distinct advantage to use the same code for both the turbulence model evaluation and plume calculations. This will rule out the influence of any code "idiosyncrasies" on plume flowfield calculations, which might be introduced if a different code were used to make flight calculations.

In what follows, we first give a brief overview of rocket and aircraft plume flowfields. Next, we discuss the turbulence models evaluated, followed by comparisons between calculations using each model and laboratory data on incompressible and compressible two-dimensional shear layers and jets, H_2/air diffusion flames, supersonic H_2/air reacting jets and liquid propellant rocket plumes. Finally, based on this evaluation, recommendations are given stating which turbulence model appears most promising for flight calculations and what future work is necessary to gain additional confidence in this model.

2. Rocket and Aircraft Plume Flowfields

Only a brief description of the plume flowfields will be given here, emphasizing: (1) the conditions under which any turbulence model must be effective, and (2) the major differences between the laboratory conditions for which most modeling "constants" are determined, and actual plume flowfields. A more detailed treatment of rocket and aircraft plume structure is given in other work by the authors.[9,12]

Underexpanded rocket plumes operating at altitudes at which afterburning occurs have completely different structure than perfectly expanded laboratory jets. Aircraft plumes, on the other hand, which are nearly perfectly expanded (i.e., nozzle exit pressure equals ambient pressure), with little afterburning (energy release) in the plume itself, are somewhat similar to laboratory jets. Figure 1a shows a schematic of the nearfield of an underexpanded rocket plume. The mixing region (including the effects of afterburning, if any) is shown superimposed on the inviscid/shock structure. There is clearly a substantial downstream distance for which the mixing region is similar to a two-dimensional shear layer. Further downstream, where the thickness of the mixing region is large compared to the inviscid plume radius, axisymmetric effects become important and the mixing region is similar to the transition region of an axisymmetric jet. Although there can be substantial pressure gradients in this flowfield, particularly in the first inviscid cell, the pressure gradient across the shear layer itself is not generally large.

Figure 1b shows, to a different scale, the plume farfield. Here the similarities to the fully developed region of an axisymmetric jet are evident; however, there are significant differences. The "true" initial conditions for the (constant pressure) plume farfield are those at the end of the nearfield, and are highly nonuniform. This is in contrast to constant pressure laboratory jets, in which essentially uniform initial conditions are specified at the nozzle exit.

Which regions of the plume are of most importance depends very strongly on the particular application. For studies keyed to the effects of the plume on vehicle design (e.g., base heating), the nearfield structure is of prime concern. In the determination of IR signatures for low altitude (i.e., less than 70 km) afterburning plumes, both nearfield and farfield contributions to the total plume signature can be significant, the precise breakdown depending on the vehicle configuration, propellant system, and flight conditions.*

Aircraft plume IR signatures[13] at 90° aspect angle (broadside), on the other hand, are directly dependent on the length of the inviscid core; i.e., the point at which the mixing region reaches the plume axis. At aspect angles near 0° (nose-on) the initial growth of the shear layer plays an important role in determining the IR signature[1]. For these applications, it is evident that the very nearfield mixing processes are important. These processes, in turn, depend on the size and profile shape of the external boundary layer on the nozzle afterbody. This situation is closely analogous to small scale laboratory jet experiments, in which a knowledge of the initial boundary layer properties is essential to the data interpretation.

*In a related study[1] the authors define plume regions making the major contribution to the IR signature for a large booster at lower (<20 to 30 km) and higher (>30 to 40 km) altitudes, within the low altitude region.

The BOAT code mentioned in Section 1 solves the axisymmetric (parabolic) jet mixing equations for a reacting gas mixture by a mixed implicit/explicit finite difference procedure in transformed (stream function coordinates). Its use of a shear layer discretization procedure makes it a good computational tool for interpreting laboratory jet data (in which initial boundary layers are usually important) and for underexpanded plume calculations. Reference 10 gives the differential and finite difference equations solved by BOAT, together with the salient features of the numerical integration, the method of treating finite-rate chemistry, and the procedure for utilizing an inviscid flowfield as input data for an overlaid calculation.

In summary, we reiterate that very significant differences are likely to exist between the laboratory test conditions under which most turbulence model constants are determined (and models are evaluated) and the full scale flowfields the models are used to predict. Because of these differences, the turbulence model used for flight calculations must be demonstrated to account for as wide a body of well documented laboratory data as possible. Only then can we gain confidence in the flight predictions. The turbulence model evaluation reported in this paper addresses itself directly to these problems.

3. Turbulence Models Evaluated

The emphasis in this study was to evaluate turbulence models which have been used for rocket and aircraft plume flowfield calculations. Two classes of models were chosen: simple eddy viscosity models and two-equation (TKE) models. We have not evaluated one-equation TKE models to date. Multi-equation models (e.g., second-order closure[33]) have been excluded from the evaluation because they are presently oriented towards fundamental research; it is not likely that they will be used in the near future for routine plume calculations.

Simple Eddy Viscosity Models

Donaldson/Gray[14] (D/G). This model extends the basic Prandtl eddy viscosity model[15] to compressible flows. A series of measurements on supersonic jets into still air were utilized together with an integral solution of the turbulent shear layer equations, to obtain an empirical correction to the eddy viscosity coefficient, K. The eddy viscosity is expressed as

$$\mu = K(M_{l_2})\rho(r_{l_2}-r_i)|U_I-U_E|/2 \qquad (1)$$

Figure 2 gives a schematic representation of r_{l_2} and the empirical correction for K as a function of M_{l_2}. The inner mixing zone boundary, r_i, in the nearfield is somewhat arbitrary. The D/G formulation utilized the exact edge of the mixing region, which is readily implemented within the framework of an integral boundary layer solution with assumed profile shapes. For use in computer codes with finite difference solutions, however, it is better to choose an inner boundary location where the velocity is some percentage of the jet velocity, u_j. In BOAT, r_i is located where $(u_j-u)/(u_j-u_e) = 0.1$. In the farfield, $r_i = 0$, the length scale is equal to the jet halfwidth, and the velocity, U_I, is the centerline velocity. In the transitional region, the results can be sensitive to the switch from nearfield to farfield formulations since δ can change abruptly. It should be noted that this model is not readily adaptable to flow situations with more than one length scale, e.g., shear layers formed from initial boundary layers.

This model is indeed the simplest of eddy viscosity formulations since it assumes that the eddy diffusivity, μ/ρ, is constant across the mixing region. In spite of this obvious limitation for application to complex exhaust plume flows, the D/G model is widely used in conjunction with the Low Altitude Plume Program[16] (LAPP)* for many applications. This is no doubt due more to its presence as a turbulence model option** within the LAPP code rather than its widespread acceptance on any fundamental basis.

An empirical correction to the D/G model, developed by Smoot,[17] has also been used for plume flowfield calculations. The correction is in the form of an additive term to the coefficient, $K(M_{l_2})$ (see Eq. (1)), and is a function of the velocity difference between the exhaust and the external stream, and the density and Mach number evaluated at the half radius. Smoot obtained this correction via an extensive correlation of core lengths measurements for nonreacting and reacting laboratory jets. The computer code used in the study was based on an integral solution to the free shear layer equations (similar to the code developed by D/G[14]). However, recent work by Rhodes[18] has indicated that when this correction factor is applied within a finite-difference formulation (i.e., in LAPP), inconsistent comparisons with compressible jet and rocket plume data are obtained. In addition, the correlation of data based on core length alone can be misleading, particularly for reacting flows. For example, Pergament and Fishburne[19] have shown good agreement between measured and calculated (via the LAPP code with the D/G model) centerline temperatures for an H_2/air diffusion flame, but very poor agreement between measured and calculated radial temperature profiles. For the above reasons this correction does not appear to contain the required generality to yield reliable aircraft/rocket plume flowfield predictions and was not evaluated in this study.

The Ting/Libby[20] (TL) variable density correction to the Prandtl eddy viscosity model has also been incorporated as an option in the LAPP code and has been used for plume flowfield calculations (e.g., Rudman[21]). The TL correction is an extension of the Mager compressible to incompressible

*LAPP is a coaxial constant pressure mixing/afterburning code which, for many years, served as the standard JANNAF Plume Model (SPM). It is being replaced by the considerably more advanced model under development at A.R.A.P.[9]. The new JANNAF SPM utilizes the BOAT code (which essentially replaces the LAPP code) as the mixing/afterburning module.

**In its standardized form, the LAPP code only contains various simplified eddy viscosity options. It does not contain the Prandtl mixing length model or the two-equation turbulence model.

transformation used in laminar boundary layers and there is no fundamental basis for its application in turbulent shear flows. Attempts to evaluate its usefulness are therefore not worth the effort.

Prandtl Mixing Length (ML)[22]. The extended version of the Prandtl mixing length model accounts for the variation of eddy viscosity across the mixing layer via its dependence on the local velocity gradient, as noted in Fig. 3. It has been evaluated against much of the data presented at the NASA/Langley Free Shear Flow Conference[2] by Rudy and Bushnell[4] and Launder et al.[7]. A preliminary assessment was made by the present authors in Ref. 23. It was chosen for evaluation in this study because of its usefulness and reasonable performance in the Shear Flow Conference Studies[2] and in applications related to nearfield jet entrainment calculations,[11] for determining aircraft boattail pressures.

Two length scale constants are required in using this mode; viz, one for the nearfield and one for the farfield, both of which are related (in the BOAT formulation) to the full thickness of the mixing layer, δ. Values of the length scale constants for this study were determined by matching the experimental data discussed in Section 4. As noted in Fig. 3 these are: ℓ/δ = 0.065 in the core region and ℓ/δ = 0.08 after the mixing layer reaches the axis. Dual length scales are implemented for shear layers with maxima or minima (i.e., shear layers formed from initial boundary layers); δ_1 and δ_2 are defined in Fig. 3 and $\ell/\delta_{1,2}$ = .065 is used.

Two Equation (TKE) Models

$k\varepsilon 2$. The $k\varepsilon 2$ model of Launder, et al.[7] was chosen for evaluation because (1) it was generally successful in predicting the incompressible flows studied in the NASA/Langley Free Shear Flows Conference[2] and (2) the work of Dash, et al.[25] showed that a compressibility-modified $k\varepsilon 2$ model gave marked improvements over the basic $k\varepsilon 2$ model for supersonic jet flows. The earlier k-W model[24] developed by the group at Imperial College was not considered in this study, although there are recent indications of some success[25] in calculating liquid propellant plume properties.

The use of differential equations for the turbulent kinetic energy and dissipation rate (related to a length scale) in the $k\varepsilon 2$ model, permit accounting for the turbulence "history" and thus provide this model with the basis for analyzing the complex plume flowfields, which is not available in simple eddy viscosity models. (The $k\varepsilon 2$ model has been used for plume calculations by Dash, et al. in Refs. 1 and 26.)

In this formulation the turbulent viscosity is given by

$$\mu_t = C_\mu \rho \frac{k^2}{\varepsilon} \qquad (2)$$

where the turbulent kinetic energy, k, and dissipation rate, ε, are obtained from the differential equations given below in x, ψ (stream function) coordinates (the equations used in BOAT),

Turbulent Kinetic Energy

$$\frac{\partial k}{\partial x} = \frac{1}{\psi}\frac{\partial}{\partial \psi}\left(\frac{A}{\sigma_k}\frac{\partial k}{\partial \psi}\right) + \frac{1}{u}(P - \varepsilon) \qquad (3)$$

Turbulent Dissipation

$$\frac{\partial \varepsilon}{\partial x} = \frac{1}{\psi}\frac{\partial}{\partial \psi}\left(\frac{A}{\sigma_\varepsilon}\frac{\partial \varepsilon}{\partial \psi}\right) + \frac{\varepsilon}{uk}\left(C_1 P - C_2 \varepsilon\right) \qquad (4)$$

where

$$A = \mu_t \frac{\rho u r^2}{\psi}$$

$$P = \frac{Au}{\psi}\left(\frac{\partial u}{\partial \psi}\right)^2$$

and the transformation from (x,r) to (x,ψ) coordinates is given by

$$\psi \frac{\partial \psi}{\partial r} = \rho u r \qquad (5)$$

$$\psi \frac{\partial \psi}{\partial x} = -\rho v r$$

C_μ and the constants C_1, C_2, σ_k, and σ_ε have been extracted directly from Reference 7. As in the ML model, the constants differ for nearfield (2D) and farfield (axisymmetric) situations. These constants are summarized below:

$$C_\mu = 0.09\ g\ (\overline{P/\varepsilon}) - 0.0534\ f$$

$$C_1 = 1.4$$

$$C_2 = 1.94 - .1336\ f$$

$$\sigma_k = 1.0$$

$$\sigma_\varepsilon = 1.3$$

$$f = \left[\frac{r_e}{2(u_e - u_c)}\left(\left|\frac{du_c}{dx}\right| - \frac{du_c}{dx}\right)\right]^{0.2}$$

where $\overline{P/\varepsilon}$ is the shear stress weighted average across the mixing region. The functional dependence of g (the "weak" shear flow correction) on $\overline{P/\varepsilon}$ and of f on the axial velocity centerline decay follow Reference 7 directly. The function g is set equal to one for $\overline{P/\varepsilon}$=1. For low values of $\overline{P/\varepsilon}$ (e.g., in the farfield decay region of jets and plumes) g increases rapidly, thus increasing the turbulent viscosity. It is important to note that the axisymmetric correction term, f, was obtained by matching data on constant pressure, nonreacting coaxial jets. For generalized plume studies where the centerline velocity additionally changes due to both pressure gradients and chemistry effects, it may be necessary to isolate the diffusive decay effect by use of a "dummy" inert species. Several new approaches[27,28] (which do not depend on the centerline decay) for extending $k\varepsilon 2$ models to axisymmetric flows are presently being investigated, and should lead to a greater degree of generality in application of this model to complex flow situations.

In use of kε models, initial profiles of k and ε are required. Such information is generally not available, and the following procedure is employed to determine these initial values. With the mean initial velocity profile known, the radial distribution of μ_t is determined from the extended ML model (Fig. 3). Calculations to date have only used $\ell/\delta = .065$ in the initialization procedure with reasonable success. However, different initial length scale constants may be required depending on the upstream "history." With the (reasonable) estimate that $k = \sqrt{|u'v'|}/0.3$, we obtain

$$k(r) = \frac{\mu_t(r)\,|\partial u/\partial r|}{0.3\rho(r)} \qquad (6)$$

Assuming that $\overline{P/\varepsilon} = 1$, gives

$$\varepsilon(r) = \frac{0.09\rho(r)k^2(r)}{\mu_t(r)} \qquad (7)$$

kε2/Compressibility Correction

This empirical correction[29] to the basic kε2 model accounts for the observed decrease in spreading rates with increasing Mach number for 2-D shear layers. The correction was developed for use in rocket plume studies at General Applied Science Laboratories (GASL)[29]. The measure of the compressibility is based on the fluctuation Mach number, evaluated from the local turbulent kinetic energy and sound speed (see Fig. 4, where k_{max} is the maximum value of the turbulent kinetic energy at each axial station and a is the local sound speed). The factor $K(M_{T_{max}})$ (extracted from Ref. 29) directly multiplies the coefficient, C_μ, reaching an asymptotic value of 0.28 at $M_{T_{max}} = 0.4$. The method used in arriving at the K factor and the inherent limitations are discussed in Section 5.

4. Incompressible Free Shear Layers and Jets

2-D Shear Layers

A detailed assessment of the turbulence models discussed above was performed by comparing predicted and observed spread rates and velocity and shear stress profiles for shear layers formed between two moving streams, including a nonsimilar shear layer (Test Case 4 of Ref. 2) with an initial profile formed by boundary layers. Fig. 5 shows that the data on spread rate variation with velocity ratio from various experimenters (as reported by Rodi[30]), have a large scatter which increases with increasing velocity ratio. This has been attributed to free stream turbulence, whose influence can be appreciable, particularly at the larger velocity ratios. The higher values of σ (lower spread rates) are therefore a better representation of an ideal flow having no turbulence in the streams, and are the better values with which to compare our calculations. The relation given by Abramovich[31], $\sigma/\sigma_0 = (1+u_2/u_1)/(1-u_2/u_1)$, is generally accepted as a good fit for the data with low free stream turbulence. The value of $\sigma_0 = 11$ is that obtained by Liepman and Laufer.[32] Both the kε2 and ML model (with $\ell/\delta = 0.065$)* fit these data quite well, but the D/G model predicts too fast a mixing rate.

*These data were in fact used to calibrate the 2-D (nearfield) constant (ℓ) for the ML model.

Note that the standard method of presenting the spread rate variation in terms of σ/σ_0 tends to mask the failure of the D/G model to predict actual spread rates.

Fig. 6 compares measured and calculated (with the kε2 model) velocity and shear stress profiles. The good agreement with these normalized profiles was also exhibited by both the ML and D/G models, when used in the BOAT code. Any computer code/turbulence model combination must account for these basic 2-D shear flow data as the first step in establishing credibility for use in more complex flow situations.

Comparisons between ML and kε2 model calculations and data on 2-D shear layers formed from initial boundary layers have been reported in a previous paper[13] concerning both the development of the BOAT code and the nearfield jet entrainment problem. Turbulence models must be able to accurately treat initial boundary layers in order to handle the nearfield of jet aircraft plumes. The velocity profile results shown in Ref. 13 indicate that both the kε2 and ML models very accurately calculate the important velocity deficit region and the subsequent development of the shear layer far downstream. As noted previously, the D/G model cannot be expected to treat shear layers formed from initial boundary layers with large mass flow deficits.

Jets into Still Air

Fig. 7 compares centerline velocity data from several investigators with model calculations. No initial conditions were specified in these data sets. The following points should be noted:

(1) These data were used to calibrate the farfield ML constant ($\ell/\delta = 0.08$). Use of the nearfield constant for the entire length of the jet gives mixing rates which are too slow.

(2) The ML model accurately predicts the core length using the value of $\ell/\delta(.065)$ determined from 2-D shear layer data.

(3) The D/G model predicts mixing rates which are too large in the nearfield. The farfield predictions however are in good agreement with the data.

(4) The kε2 model does not agree at all with the data. The reason for this (as shall be brought out more clearly in subsequent comparisons) is <u>not</u> the failure of the kε2 model, but a lack of knowledge of the initial mean velocity profiles. Without this knowledge we initialized the calculations using "top hat" velocity profiles (as we did for the ML and D/G models), with the poor results noted. The important point to be noted here is that when using this more sophisticated turbulence model, reasonably correct initial values of k and ε must be specified. The initialization procedure for k and ε given by Eqs. (6)

*Some particularly important applications are, nozzle afterbody drag and near nose-on IR radiation.

and (7) requires a knowledge of the mean velocity profile. If this is not known, and the magnitude of the velocity defect is significantly large, the resulting flowfield calculations are likely to result in initial mixing rates which are too slow* (initial viscosity too small). On the other hand the simple eddy viscosity models are less sensitive to a lack of knowledge of initial conditions.

Figure 8 compares jet spread data with the model calculations while Fig. 9 shows normalized velocity profiles in the farfield, self-preserving regions of the jet (i.e., $> x/r_j = 100$). Here we note that the D/G model does not produce an accurate profile shape.

Comparisons are next made between the data from Test Case 6 of the NASA/Langley Free Shear Flows Conference[2] and the model calculations. Fig. 10 gives initial normalized viscosity profiles, calculated from the initial velocity profile (specified at $x/r_j=2$) and Eqs. (6) and (7). Also shown for comparison is the initial constant value of Launder, et al.[7] This should be contrasted with the profile for Test Case 9 (to be discussed in the next section) which is specified directly at the jet exit and clearly shows the minimum in viscosity caused by the velocity deficit in the initial boundary layers.

Fig. 11 compares the model predictions with the data, showing that the $k\varepsilon 2$ model does an excellent job for this case with well-defined initial conditions. Again, the D/G model predicts too short a core length and predicts mixing that is too slow in the farfield (as indicated by the measured and predicted shapes). For some inexplicable reason, the ML model does quite poorly for this case. In order to test the effect of initial conditions on the $k\varepsilon 2$ model predictions, initial values of the turbulent viscosity across the jet were arbitrarily increased and decreased by a factor of 5. (This also changes the initial values of k and ε by factors of 5.) The extreme sensitivity noted to initial viscosity is not surprising because the initial profiles are specified far from the jet exit ($x/r_j=2$), and the initial shear layer is large compared to the exit diameter.

It should be noted that in the approach of Launder, et al.[7] initial values of viscosity are varied until the measured core length is correctly predicted. All $k\varepsilon 2$ model calculations reported here employed the "fixed" initialization procedure described in Section 3, which requires no a priori knowledge of the "solution" (i.e., the actual core length).

Air Jets into Moving Streams

The data of Test Case 9 of Ref. 2 have been used to evaluate the models for concentric, coflowing streams. Fig. 12 shows that the centerline velocity decay predicted by the $k\varepsilon 2$ model is in excellent agreement with the data, including both the core length and farfield slope. This case shows much less sensitivity to the variation in initial turbulent viscosity than Test Case 6, due, no doubt, to the relatively smaller initial boundary layers. Both the D/G and ML models underpredict the core length, while both exhibit the correct farfield decay.

Since the simple eddy viscosity models undergo an "abrupt" transition from nearfield to farfield constants, it is expected that they will not be able to accurately predict flow in the transitional region (for this case, from $5 < x/D < 30$). In this region, the turbulence processes are well out of equilibrium and these simple models are predicted upon equilibrium turbulence assumptions. The $k\varepsilon 2$ model, on the other hand, which accounts for the turbulence "history" does admirably in analyzing the nearfield, farfield, and transitional regions.

Summary of Incompressible Shear Layer and Jet Results

From the comparisons between model predictions and data shown in this section we observe that

(1) Both the $k\varepsilon 2$ and ML models yield predictions consistent with the 2-D shear layer spread rate and profile data. The D/G model yields spread rates which are too large.

(2) Both the $k\varepsilon 2$ and ML models accurately predict a shear layer produced from initial boundary layers (see Ref. 13).

(3) Predictions with the $k\varepsilon 2$ model are, overall, in good agreement with the incompressible jet data, provided that reasonable values of the initial turbulent viscosity are utilized. The D/G model generally underpredicts the core length, giving mixing rates which are initially too large. In the farfield, predicted mixing rates are generally too small. The ML model fares only slightly better than the D/G model for these cases.

5. Compressible Free Shear Layers and Jets

2-D Shear Layers

The experimental data which demonstrate the decrease in spread rates with increasing Mach number for two-dimensional shear layers are given in Fig. 13. The dashed curve represents a best fit of the data, as recommended by the NASA/Langley Shear Flows Conference Evaluation Committee,[2] (The Hill and Page (1969) data are for low Reynolds numbers). BOAT calculations with the $k\varepsilon 2$ model are shown at $M_1 = 1,4$ and 5 and indicate the failure of the basic model to handle compressibility effects. These results are seen to be consistent with those of Launder, et al.,[7] using the GENMIX code.

In Section 3 we discussed the compressibility correction to the $k\varepsilon 2$ model developed by Dash, et

*This is much more important in the interpretation of small-scale laboratory data, where initial boundary layer displacement and momentum thicknesses are relatively large (compared to the jet diameter), than for rocket exhausts where the initial boundary layer is likely to be relatively small.

al.,[29] at GASL. The form of $K(M_{t_{max}})$, given in Fig. 4, was determined by matching the data given in Fig. 13 at $M_j = 1, 2$ and 4 (utilizing a trial and error procedure). Since this empirical correction is based on a property of the turbulence, i.e., the Mach number based on turbulent fluctuations, it offers some promise for use in more generalized flow situations,* demonstrated in Ref. 29. Based on that work, we decided to evaluate this $k\varepsilon2$, compressibility corrected model as part of the present study.

Figure 14 compares the spread rate data given in Fig. 13 with calculations using BOAT, incorporating the compressibility corrected $k\varepsilon2$ model. It is noted that the BOAT results start to diverge from the data at Mach numbers greater than 2, although at Mach 3 the agreement is still reasonable. The discrepancy between the BOAT and GASL results (which used the CHEMX code[34]) at Mach 4 could possibly reflect some fundamental differences between the BOAT and CHEMX codes. At this point the reasons for the difference are not clear. The predicted asymptotic spread rate calculated by BOAT is $\sigma \approx 23$, while the only two available pieces of data at Mach numbers higher than 3 range from $\sigma = 34$ at Mach 4 to $\sigma = 38$ at Mach 5. It is clear that by adjusting the $K(M_{t_{max}})$ curve of Fig. 4 to give lower values of K for $M > 0.3$ the higher Mach number data could be matched exactly. However, considering that (1) there is a paucity of 2-D shear layer data at Mach numbers greater than 2 and (2) there are no available axisymmetric jet data for Mach numbers greater than about 2.5, this correction will not be "fine-tuned" to BOAT until after all the remaining compressible jet (nonreacting and reacting) data are studied.

Regarding the relevance of the compressible shear layer data to aircraft and rocket plumes, the following points should be noted:

(1) The data are for the limiting case of one stream mixing with another at zero velocity.

(2) The data are all supposed to be for isoenergetic flows, where the stagnation enthalpy of the jet and freestream are equal. This implies that the freestream temperature is greater than the jet temperature, e.g., for $T_j = 110^oK$ and $M_j = 3$, $T_e = 208^oK$; for $M_j = 5$, $T_e = 660^oK$.

(3) Aircraft and rocket plumes are not isoenergetic. In plumes, the high velocity exhaust is at a higher temperature than the freestream, in contrast to the test conditions of Fig. 13.

(4) Most of the data are in the $1 < M_j < 2$ range. There is only one data point at $M_j = 4$ and $M_j = 5$. Thus, the asymptotic nature of the "recommended" curve may be questionable.

*It should be noted that the correction is formulated so that the $k\varepsilon2$ (comp. corr.) model reduces to the basic $k\varepsilon2$ model for incompressible flows.

Jets into Still Air

Figure 15 compares predicted and measured centerline velocity decays for a Mach 2.2 air jet into still air. Both eddy viscosity models show the same poor agreement with the data (initial mixing is too fast) as they did for the incompressible jet of Fig. 11. The basic $k\varepsilon2$ model also gives mixing rates which are initially too fast,* in marked contrast to its success in predicting incompressible jets. This result can be interpreted in the same way as the 2-D shear layer results of Fig. 13, i.e., the $k\varepsilon2$ (incompressible) model overpredicts the mixing rate for this compressible flow. Although the core length is slightly overpredicted, the compressibility corrected $k\varepsilon2$ model gives results in much better overall agreement with the data. Figure 16 compares predicted and measured radial profiles at two axial stations; $x/r_j = 8$ is in the core region while $x/r_j = 27$ is in the transition region. The performance of the $k\varepsilon2$ (comp. correct) model which follows the data points quite closely is particularly impressive.

It should be pointed out that these Mach 2.2 air jet data are still the standard for testing turbulence models under conditions where compressibility effects are important. There is a scarcity of good data in this flow regime, particularly with supersonic external streams.

H_2/air Jets

Test case 12 of the NASA/Langley Shear Flows Conference[2] provides a test of the models for relatively mild compressibility effects, but with two streams of widely different density. Figure 17 shows centerline decays of velocity and H_2 mass fraction. Examining the eddy viscosity model results first, we note that the D/G model initially mixes too slow, in contrast to its performance for all the incompressible and compressible air/air shear layers and jets studied to date. The ML model shows quite reasonable agreement with these data, particularly in predicting the core length and initial rate of decay. The $k\varepsilon2$ (comp. correct) model underpredicts the core length but overall is in reasonable agreement with the data (sensitivity of the results to initial turbulence levels was not studied in this case**). Figure 18 shows that the ML model gives good overall agreement with the data, particularly at the downstream station, while the $k\varepsilon2$ (comp. correct) model produces only fair results. The D/G model does not follow the trend of the data at all.

Summary of Compressible Free Shear Layer and Jet Results

The failure of the basic $k\varepsilon2$ model to calculate air/air free shear layers and axisymmetric jets with marked compressibility effects has been noted. This (incompressible) model does not

*Reducing the initial values of turbulent viscosity by a factor of 5 does not substantially reduce the initial mixing rates, the results being similar to those shown in Fig. 12.

**Evans, et al.[6], using the basic $k\varepsilon2$ model, show that the data can be matched reasonably well by varying the initial viscosity levels.

predict the observed decrease in mixing rates with increasing Mach number. The incorporation of a compressibility correction, correlated with a fluctuating Mach number based on turbulent kinetic energy, has been shown to give much better agreement with the Mach 2.2 air jet data. Both the D/G and ML eddy viscosity models overpredict the initial mixing rates for the compressible air jets, as they did for the incompressible air jets. For the H_2/air jet studied the situation is quite different. Here the D/G model drastically underpredicts the initial centerline velocity decay while the ML model is in good overall agreement with the data. The $k\varepsilon 2$ (comp. correct.) model does not fare as well as it did for the homogeneous jets.

These incompressible and compressible jet results clearly demonstrate the inconsistency of the eddy viscosity models tested. Except for the ML model applied to test case 12 of Ref. 2, the models generally do not agree with the data. A slight inconsistency is also noted with the $k\varepsilon 2$ model for the H_2/air jet. However, the model has still performed reasonably well on the wide variety of cases studied.

6. Reacting Jets

H_2/Air Subsonic Streams

An excellent data base for low speed reacting jets has been obtained by Kent and Bilger.[34] In these experiments a cold H_2 jet (7.6×10^{-3}m dia.) at a velocity of 178 m/sec was injected into a coflowing airstream at a velocity of 15 m/sec, and ignited by a pilot flame. The data have been widely used for comparison with a number of models of turbulent chemically reacting jets (e.g., Refs. 6, 19, 35), and are now a "standard" for evaluating turbulence models in reacting flow codes. A standard H_2/O_2 8-step reaction mechanism (see, e.g., Ref. 19) was incorporated into the BOAT code for these calculations.

Figure 19 compares predicted centerline temperatures with the data. In a similar manner to the nonreacting H_2/Air jet the D/G model predicts mixing rates which are much too slow. The $k\varepsilon 2$ model, on the other hand, gives results in good agreement with the data, although the predicted peak temperature is somewhat high. The effect of varying the turbulent Prandtl number from .85 to 1.0 is seen to be negligible.* Fig. 20 shows the excellent agreement between predicted (using the $k\varepsilon 2$ model) and measured radial temperature profiles. Of particular note is the good prediction of the profile widths at the three axial stations. The D/G model is seen to fail miserably in this regard. No calculations have been made for the ML model.

*The turbulent Prandtl number (Pr) is generally assumed to be in the range from 0.7 to 1.0. The sensitivity of liquid propellant plume calculations to the choice of Pr is demonstrated in Refs. 1 and 23.

H_2/Air Supersonic Streams

The recent work of Evans, et al.[6] at NASA/Langley reports on a new set of supersonic reacting jet data taken by Beach, which have been used in this turbulence model evaluation. In addition, Evans made a parametric set of calculations using a code developed by Spalding, et al.[36] containing the $k\varepsilon 1$ model*. Chemistry was treated by either: (1) a global kinetic scheme incorporating an eddy breakup model to account for the effects of fuel/oxidizer "unmixedness" or (2) an equilibrium chemistry (complete reaction) scheme. The conditions of these experiments were:

	H_2 Jet	Free Stream
Mach Number	2.0	1.9
Temperature, °K	250	1500
Velocity, ft/sec	7980	4950
Pressure, atm.	1.0	1.0
Mass Fraction		
H_2	1.0	0
O_2	0	.241
N_2	0	.478
H_2O	0	.281

Note that the H_2 jet mixes with a hot "vitiated" air stream and ignition takes place in much the same manner as in an afterburning rocket plume. Except here the temperature ratio is the inverse of that for an afterburning plume. Initial velocity and temperature profiles were measured and used as input to the calculations. Relatively large initial boundary layer effects were noted from the initial velocity profiles.

Figure 21 compares measured and predicted centerline H_2 mass fractions. These results show the poorest agreement for the D/G model, which drastically underestimates the decay rate. More reasonable agreement is obtained with the other models, with both ML and $k\varepsilon 2$ models following the trend of the data. No significant influence of compressibility is given by the GASL correction, while the influence of Pr changes the results by roughly 20%. One calculation was made to test the influence of initial viscosity, by varying ℓ/δ the initial length scale. Thus the value $\ell/\delta = 0.016$ shown in Fig. 21 is 1/4 the value used in the standard calculations, reducing the initial viscosities by a factor of 16. The results shown are consistent with the calculations of Evans[6] regarding the magnitude of the reduction in decay rate that results from this decrease in initial length scale.

Figures 22a-d show show radial mole fraction profiles of H_2, O_2, N_2, and H_2O at $x/r_j = 31$. A consistent picture emerges from a study of all profiles. All models except the D/G model do not adequately account for the rate at which H_2 and and O_2 mix (and react). The differences in predicted radial profiles among the other models are relatively small. These results are in stark contrast to those shown in Fig. 21, which appear to indicate the failure of the D/G model for this situation. This emphasizes the very important

*This is the $k\varepsilon 2$ model without the "weak" shear flow correction.

point (noted earlier) regarding comparisons between model calculations and data for reacting flows; i.e., comparisons between predicted and measured centerline values alone are not sufficient to indicate the validity of a turbulence model.

Why does the D/G model emerge in this situation as the only model to predict with reasonable accuracy the radial transport of fuel and oxidizer? The answer is far from clear, particularly in view of the failure of the D/G model to adequately account for much of the nonreacting data presented here, and the radial temperature profiles for the subsonic reacting H_2/air jets (Fig. 20). At this point we can only speculate about the reasons, but considering the history of the D/G model shown in this paper it would appear that this result is fortuitous. Rather than dwell on the D/G model, what is needed is to understand why the $k\varepsilon 2$ model does not do well for this supersonic reacting jet. The combination of supersonic flow and H_2/O_2 reactions is apparently not adequately treated by the compressibility corrected $k\varepsilon 2$ model, even though the model is quite reasonable for nonreacting supersonic flows and subsonic flows with fast chemical reactions. Since afterburning rocket plumes are, in fact, supersonic chemically reacting flows, it is imperative that this problem be resolved. Only then can a fair measure of confidence be gained in flight calculations and a true generalized predictive capability be established.

Figure 22e compares the present finite rate chemistry calculations with those of Evans[6] for the case of complete chemical reaction and Pr = 0.7. The basic similarity between the two calculations is noted, the major difference being that the equilibrium chemistry calculations drastically overpredict the peak H_2O levels, i.e., even at 1 atm pressure, finite rate calculations perform better than the local equilibrium assumption. Evans' results using the eddy-breakup model (not shown here) do not account for the measured H_2O peak.

7. Rocket Plumes

There are few carefully controlled experiments on laboratory rocket exhausts which are suitable for use as part of a turbulence model evaluation. One such data set has been obtained as part of a test series conducted at AEDC.[37] In this experiment on a (nearly) perfectly expanded liquid propellant plume, measurements of pitot pressure and carbon to nitrogen mass ratios were obtained. Initial conditions for this test case (nozzle exit Mach number 3.4; freestream Mach number 2.0) are given in Ref. 37, together with the complete set of test data.

The slight degree of underexpansion (P_j = .337 atm; P_e = .26 atm) was treated via an isentropic expansion from exit to ambient pressure, thus determining the velocity and temperature and the (larger) area required to pass the rocket exhaust flow. The chemical reaction mechanism incorporated into BOAT for these calculations was the H_2/O_2 mechanism of Ref. 19 with the addition of the dominant reactions accounting for the conversion of CO to CO_2 ($CO + OH \rightleftarrows CO_2 + H$ and $CO + O + M \rightleftarrows CO_2 + M$). The rate coefficients of Ref. 38 were employed for these calculations.

Fig. 23 shows predicted centerline temperature and velocity distributions using both the $k\varepsilon 2$ and $k\varepsilon 2$ (comp. correct.) models. The differences are seen to be quite large; the compressibility correction reducing the mixing rate rather drastically for this high Mach number flow with rather mild afterburning.* Noted on the figure are the axial locations where the C/N ratio was measured. At the first station ($x/r_j \approx 21$ or $x = 3$ ft) the $k\varepsilon 2$ (comp. correct.) model predicts that the mixing region has not yet reached the axis, thus the axis value of C/N will be the combustion chamber value. The basic $k\varepsilon 2$ model, on the other hand, will show a decay in C/N. This is clearly shown in Fig. 24, which plots C/N ratio as a function of radial distance, at the three axial stations. Indeed, we note that at $x = 3$ ft, the $k\varepsilon 2$ (comp. correct.) curve fits the data quite well while the basic $k\varepsilon 2$ model fails to account for the reduced mixing rate due to high Mach number. However, at the two downstream stations, the measured decay of C/N is greater than that predicted by the compressibility corrected model. This is evident even though the scatter of the data gets increasingly larger as the absolute value decreases. (See References 18 and 37 for a discussion of error bands on these data.)

This problem may be a general one in application of the compressibility corrected $k\varepsilon 2$ model since, for the Mach 2.2 air jet, it appeared that the predicted velocity decay was too slow (Fig. 15). One possible improvement to the compressibility correction would be to have separate nearfield and farfield corrections. This would be a consistent approach, since the $K(M_{\tau_{max}})$ correction was obtained from 2-D shear layers only, and may be applicable only in the nearfield. A separate factor could then be empirically determined from the available data (in a similar manner to the way $K(M_{\tau_{max}})$ was determined), and applied to the farfield. Thus, the form of C_μ would become,

$$C_\mu = 0.09\, K_1(M_{\tau_{max}})\, g(\overline{P/\varepsilon}) - .0534\, K_2(M_{\tau_{max}})\, f$$

K_2 would therefore only become effective when $du_c/dx < 0$ (see the definition of f on p. 4).

8. Concluding Remarks

This work was motivated by the need to determine what turbulence model or models appear to offer the most generalized predictive capability for aircraft and rocket plume flowfields. The approach taken was to systematically compare turbulence model predictions, within one computer code (BOAT), with a broad range of well documented laboratory data on incompressible and compressible 2-D shear layers and jets, and chemically reacting jets and plumes. This is necessary because of the lack of flight data on plumes which can

*The fuel content of the exhaust is roughly 13 mole % H_2 and 11 mole % CO. Thus, afterburning is "mild" in comparison to either the supersonic H_2/air reacting jet discussed in Section 6 or typcial solid propellant exhausts which can contain $\approx$ 30 % H_2 and $\approx$ 20 % CO.

be interpreted in terms of the validity of any turbulence model. The models chosen were those which have been widely used for plume flowfield calculations.

Although additional data sets and (possibly) additional models remain to be investigated, some observations and conclusions that can be made from the results to date are:

1. The Donaldson/Gray eddy viscosity model performs in an extremely inconsistent manner for the incompressible shear layer and jet cases for which it is supposed to be adequate. Initial rates of mixing are too fast and farfield decay rates somewhat soo slow. For the H_2/air nonreacting jet this trend is reversed; i.e., nearfield mixing rates are much too slow. For the supersonic reacting H_2/air jet, however, the D/G model accounts quite well (the best of all models) for the measured radial species mole fraction profiles, although the centerline values are poorly predicted.

In view of its demonstrated inconsistency we conclude that the D/G model cannot be counted on for generalized plume calculations with any degree of reliability, and recommend that its usage be limited.

2. The extended form of the Prandtl Mixing Length model performs about the same as the D/G model for the incompressible jets; however, it does the best of all models in matching the H_2/air nonreacting jet data. In contrast to the D/G model, however, the ML model does not adequately predict the radial profiles for the H_2/air supersonic reacting jet. The use of this model for plume calculations should also be limited.

3. The $k\varepsilon 2$ model performs best overall for the incompressible shear layers and jets and, with the addition of a compressibility correction based on a Mach number of the turbulent fluctuations, also adequately predicts the nonreacting compressible jet data. It gives excellent agreement with the subsonic reacting H_2/air data but fails to accurately predict radial species profiles for the supersonic reacting H_2/air jets. The $k\varepsilon 2$ (compressibility corrected) model adequately predicts the nearfield C/N ratios measured in the AEDC tests on liquid propellant rocket plumes, but predicts too slow a rate of mixing in the transitional and developed regions.

Based on this evaluation, and because of its ability to account for a "history" of the turbulence via the solution of differential equations for the turbulent kinetic energy and length scale, we conclude that the $k\varepsilon 2$ model shows considerable promise for use in generalized rocket and aircraft plume calculations. However, additional work is required in order to further validate and optimize its use in flowfield models.

The use of separate nearfield and farfield compressibility corrections, as suggested in Section 7, appears to be a rational approach and consistent with the generally accepted practice of specifying nearfield and farfield turbulence model "constants".

An apparent interaction between high Mach numbers and highly energetic reactions that is not accounted for within the framework of the $k\varepsilon 2$ model is suggested by:

- The success of the basic model in accounting for data on a subsonic reacting H_2/air jet.
- The success of the compressibility corrected model in accounting for data in a supersonic (air-air) jet.
- The failure of the compressibility corrected model to account for data on a supersonic reacting H_2/air jet.

Accounting for this interaction via an empirical correction to the $k\varepsilon 2$ model requires additional data comparisons and considerably more study.

NOMENCLATURE

C_1, C_2	Constants in kε2 model
C_u	Turbulent viscosity coefficient in kε2 model (see Eq. (2))
k	Turbulent kinetic energy
$K(M_{T_{max}})$	Compressibility correction to kε2 model
$K(M_{T_2})$	Eddy viscosity coefficient, see Eq. (1)
ℓ	Turbulent length scale in ML model, see Fig. 3
$r_{0.1}$	Value of r where $(u-u_e)/(u_1-u_e) = 0.1$
$r_{0.9}$	Value of r where $(u-u_e)/u_1-u_e) = 0.9$
r	Radial distance from axis
u_2	Velocity at upper edge of shear layer
u_1	Velocity at lower edge of shear layer
u_c	Centerline velocity
U,u	Axial velocity
$\overline{u'v'}$	Turbulent shear stress
v	Radial velocity
x	Axial distance
x_c	Core length
$\bar{\delta}$	Turbulent length scale for D/G model (see Fig. 2); also thickness of mixing zone for ML model (see Fig. 3)
σ_k	Prandtl number for turbulent kinetic energy
σ_ϵ	Prandtl number for turbulent dissipation
σ_o	Value of σ for $u_2/u_1 = 0$
σ	Spread rate parameter, defined by $\sigma = 1.855\ \Delta x/\Delta(r_{0.1} - r_{0.9})$
ϵ	Turbulent dissipation rate
μ_t	Eddy viscosity
ψ	Stream function, defined by Eq. (5)
$\psi_1(x)$	Stream function at lower mixing zone boundary
$\psi_2(x)$	Stream function at upper mixing zone boundary
ρ	density

Subscripts

½	Half radius, value at radial location where $U = (U_1 + U_E)/2$
i	Inner mixing zone boundary
1	Lower boundary of mixing region
E,e	Freestream; upper boundary of mixing region
j	Jet

REFERENCES

[1] Dash, S.M., Pearce, B.E., Pergament, H.S. and Fishburne, E.S., "The Prediction of Rocket and Aircraft Exhaust Plume Structure: Requirements in IR Radiation Signature Studies," AIAA Paper 79-0095 Presented at AIAA 17th Aerospace Sciences Meeting, New Orleans, LA, 15-17 January 1979.

[2] "Free Turbulent Shear Flows," NASA/Langley Research Center, Conference Proceedings, NASA SP-321, 1972.

[3] Harsha, P.T., "Prediction of Free Turbulent Mixing Using a Turbulent Kinetic Energy Method," Free Turbulent Shear Flows, NASA SP-321, 1972, pp. 463-522.

[4] Rudy, D.H. and Bushnell, D.M., "A Rational Approach to the Use of Prandtl's Mixing Length Model in Free Turbulent Shear Flow Calculations," Free Turbulent Shear Flows, NASA SP-321, 1972, pp. 67-138.

[5] Peters, C.E. and Phares, W.J., "An Integral Turbulent Kinetic Energy Analysis of Free Shear Flows," Free Turbulent Shear Flows, NASA SP-321, 1972, pp. 577-628.

[6] Evans, J.S., Schexnayder, C.J. Jr., Beach, H.L. Jr., "Application of a Two-Dimensional Parabolic Computer Program to Prediction of Turbulent Reacting Flows," NASA Technical Paper 1169, March 1978.

[7] Launder, B.E., Morse, A., Rodi, W., and Spalding, D.B., "Prediction of Free Shear Flows--A Comparison of The Performance of Six Turbulent Models," Free Turbulent Shear Flows, NASA SP-321, 1972, pp. 361-426.

[8] Harsha, P.T., "Kinetic Energy Methods," in Handbook of Turbulence, Vol. 1: Fundamentals and Applications (Plenum Press, New York, 1977), pp. 187-232.

[9] Dash, S.M., Pergament, H.S. and Thorpe, R.D., "A Modular Approach for the Coupling of Viscous and Inviscid Processes in Exhaust Plume Flows," AIAA Paper 79-0150, presented at AIAA 17th Aerospace Sciences Meeting, New Orleans, LA, 15-17 January 1979.

[10] Dash, S.M. and Pergament, H.S., "A Computational Model for the Prediction of Jet Entrainment in the Vicinity of Nozzle Boattails (The BOAT Code)," NASA CR-3075, 1978.

[11] Dash, S.M., Wilmoth, R.G., and Pergament, H.S., "Prediction of Nearfield Jet Entrainment by an Interactive Mixing/Afterburning Model," AIAA Paper No. 78-1189, Seattle, WA, July 1978.

[12] Dash, S.M. and Pergament, H.S., "The Analysis of Low Altitude Rocket and Aircraft Plume Flowfields: Modeling Requirements and Procedures," Proceedings of the JANNAF 10th Plume Technology Meeting, CPIA Pub. 291, Vol. I, 1977, pp. 53-132.

[13] Fishburne, E.S., Pearce, B.E. and Pergament, H.S., "The Naval Weapons Center Target Signature Code. Part II." IR Radiation for Broadside (STARAD) and Near Nose-on (AARAD) Aspect Angles, A.R.A.P. Report No. (in preparation).

[14] Donaldson, C. duP. and Gray, K.E., "Theoretical and Experimental Investigation of the Compressible Free Mixing of Two Dissimilar Gases," AIAA J., Vol. 4, 1966, pp. 2017-2025.

[15] Schlicting H., Boundary Layer Theory (Pergamon Press, New York, 1955), p. 588.

[16] Mikatarian, R.R., Kau, C.J., and Pergament, H.S., "A Fast Computer Program for Nonequilibrium Rocket Plume Predictions," AFRPL-TR-72-94, August 1972.

[17] Smoot, L.D., "Turbulent Mixing Coefficients for Compressible Coaxial Submerged and Coflowing Jets," AIAA J., Vol. 12, December 1976, pp. 1699-1705.

[18] Rhodes, R.P., "Preliminary Gas Dynamic Analysis of Rocket Plumes with Subsonic and Supersonic External Airflow," AEDC-TR-76-137, November 1977.

[19] Pergament, H.S. and Fishburne, E.S., "Influence of Buoyancy on Turbulent Hydrogen/Air Diffusion Flames," Combustion Science and Technology, Vol. 18, 1978, pp. 127-137.

[20] Ting, L. and Libby, P.A., "Remarks on the Eddy Viscosity in Compressible Mixing Flows," Journal of Aerospace Sciences, October 1960, pp. 797-798.

[21] Rudman, S. and DelGuidice, P., "Multinozzle Plume Flow Fields: Structure and Modeling," JANNAF 10th Plume Technology Meeting, Vol. I, CPIA Publication 291, December 1977, pp. 277-292.

[22] Schlicting, H., Boundary Layer Theory (Pergamon Press, New York, 1955), p. 386.

[23] Pergament, H.S., Dash, S.M., and Fishburne, E.S., "Methodology for the Evaluation of Turbulence Models for Afterburning Rocket and Aircraft Plumes," Proceedings of the JANNAF 10th Plume Technology Meeting, CPIA Pub. 291, Vol. I, 1977, pp. 133-172.

[24] Rodi, W. and Spalding, D.S., "A Two-Parameter Model of Turbulence and its Application to Free Jets," Wärme Stoffübertrag, 3, 85-95 (1970).

[25] Byrd, M., Air Force Rocket Propulsion Laboratory, Private Communication, Sept. 1978.

[26] Dash, S., Boccio, J., and Weilerstein, G., "A Computational System for the Prediction of Low Altitude Rocket Plume Flowfields: Volume I - Integrated System; Volume II - Inviscid Plume Model (MAXIPLUM); Volume III - Mixing/Afterburning Model (CHEMX)," General Applied Science Laboratories, Inc., Westbury, NY, TR-239, December 1976.

[27] Pope, S.B., "An Explanation of the Turbulent Round Jet/Plane Jet Anamoly," AIAA Journal, Vol. 16, March 1978, pp. 279-281.

[28] Chien, S.C., "Numerical Computation of Subsonic Conical Diffusion Flows with Nonuniform Turbulent Inlet Conditions," AEDC TR-77-78," September 1977.

[29] Dash, S., Weilerstein, G., and Vaglio-Laurin, R., "Compressibility Effects in Free Turbulent Shear Flows," Air Force Office of Scientific Research, TR-75-1436, August 1975.

[30] Rodi, W., "A Review of Experimental Data of Uniform Density Free Turbulent Boundary Layers," in Studies in Convection, Vol. I, Ed. B.E. Launder, Academic Press, London, 1975, pp. 79-166.

[31] Abramovich, G.N., The Theory of Turbulent Jets, M.I.T. Press, Cambridge, MA, 1963.

[32] Liepman, H.W. and Laufer, J., "Investigations of Free Turbulent Mixing," NACA TN 1257, 1947.

[33] Varma, A.K. and Fishburne, E.S., "Second-order Closure Calculation of Turbulent Reacting Flows," JANNAF 9th Plume Technology Meeting, CPIA Publication 277, April 1976, pp. 47-64.

[34] Kent, J.H. and Bilger, R.W., "Turbulent Diffusion Flames," TN F-37, Dept. Mech. Eng., University of Sydney, Australia, October 1972.

[35] Rhodes, R.P., Harsha, P.T. and Peters, C.E., "Turbulent Kinetic Energy Analyses of Hydrogen-Air Diffusion Flames," Acta Astronautica, Vol. I, 1974, pp. 443-470.

[36] Spalding, D.B., Launder, B.E., Morse, A.P., and Maples, G., "Combustion of Hydrogen-Air Jets in Local Chemical Equilibrium (A Guide to the CHARNAL Computer Program)" NASA CR-2407, 1974; see also, Elghobashi, S. and Spalding, D.B., "Equilibrium Chemical Reaction of Supersonic Hydrogen-Air Jets (The ALMA Computer Program), NASA CR-2725, 1977.

[37] Nelius, M.A., Darlington, C.R., and Wasson, R.A., "Exhaust Plume Gas Dynamic and Radiation Measurements on a 500 lbf Thrust Liquid Rocket Engine at Simulated Flight Conditions," Part I, AEDC-TR-77-44, July 1977.

[38] Jensen, D.E. and Jones, G.A., "Reaction Rate Coefficients for Flame Calculations," PERME (Westcott, England), Technical Report No. 35, May 1977.

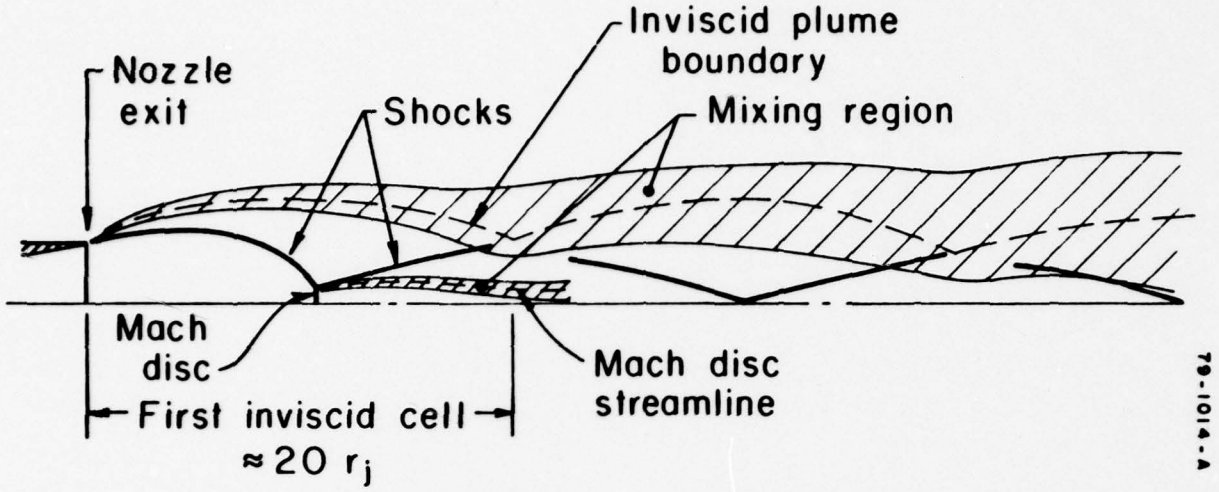

Figure 1a. Schematic of underexpanded rocket plume nearfield.

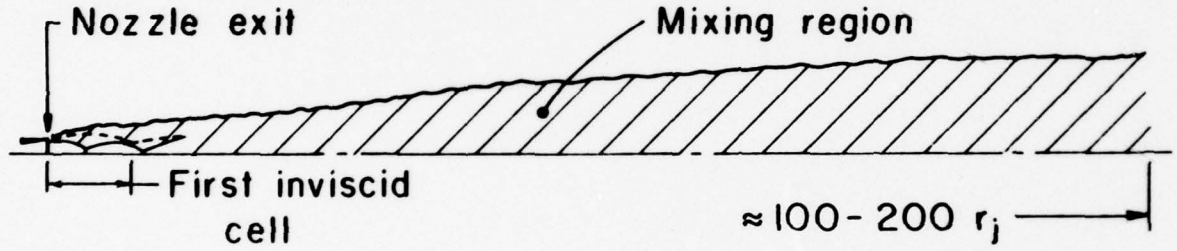

Figure 1b. Schematic of underexpanded rocket plume farfield.

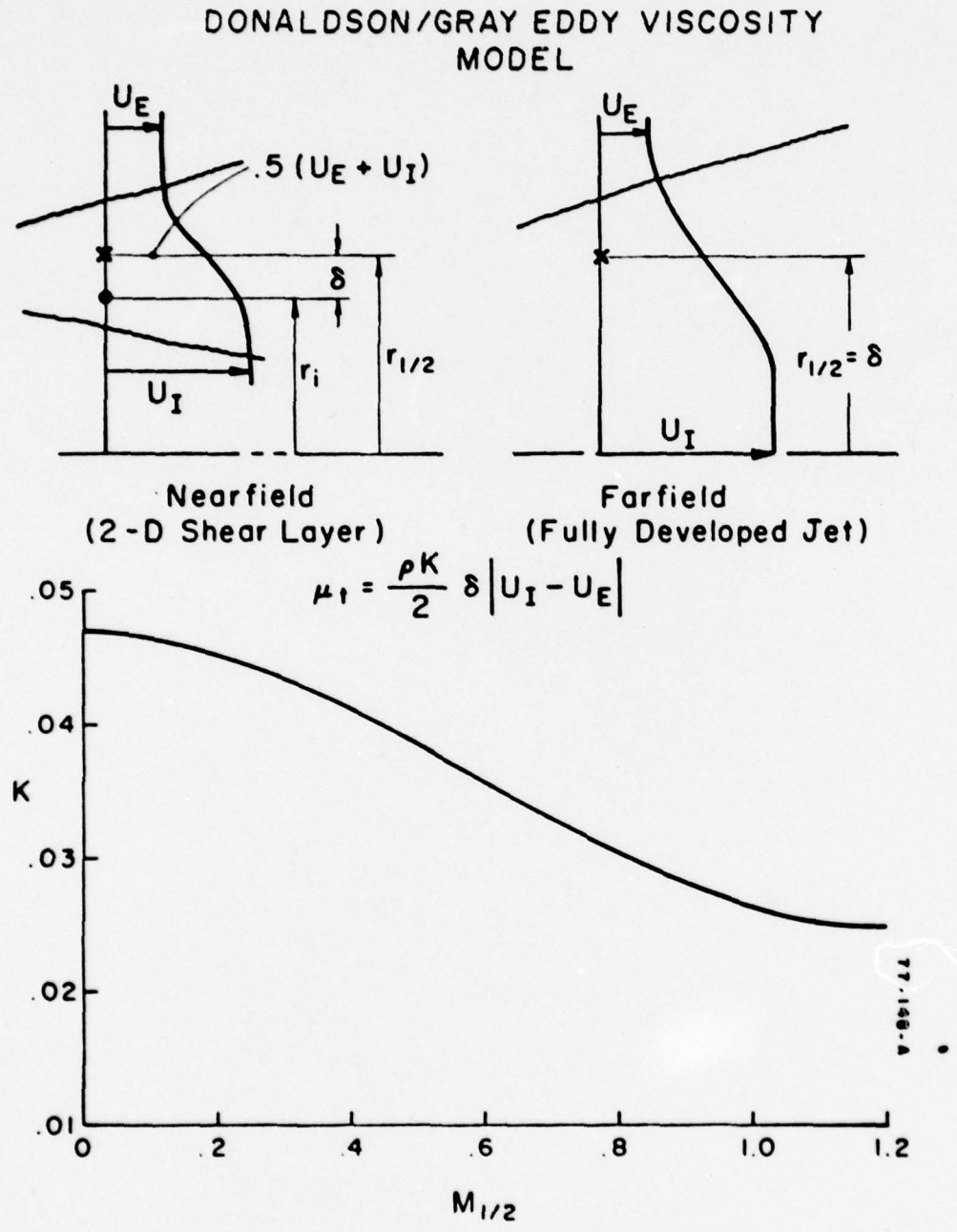

Figure 2. Donaldson/Gray eddy viscosity model formulation.

PRANDTL MIXING LENGTH MODEL

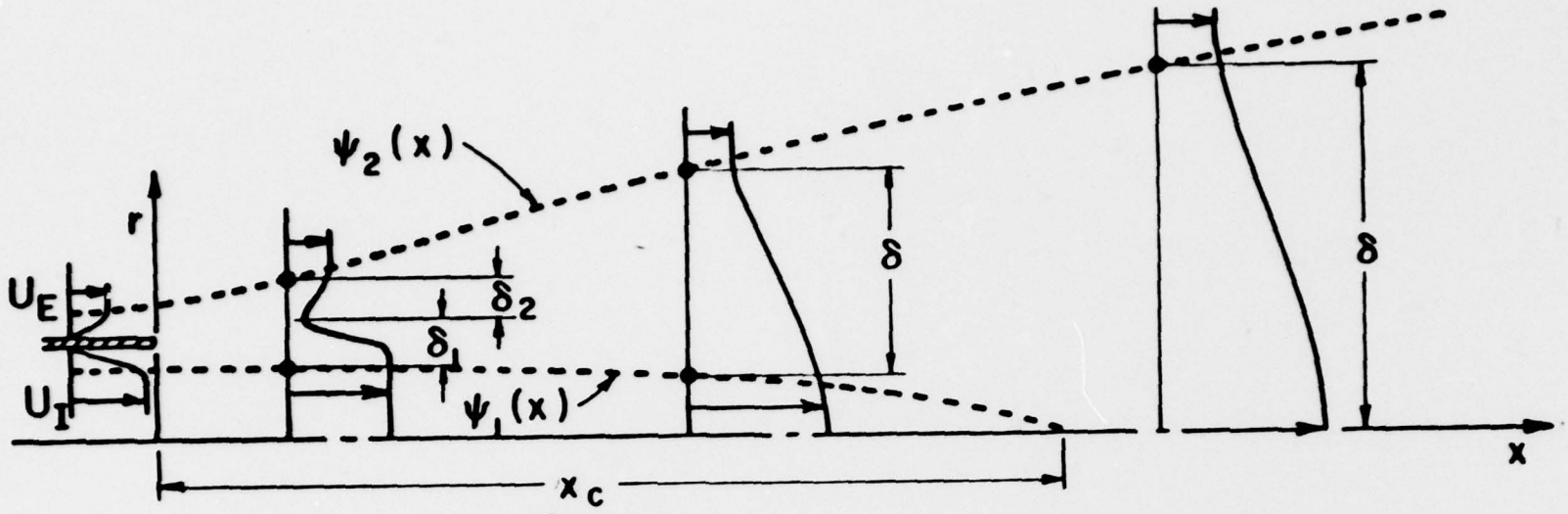

$$\mu_t = \rho \ell^2 |\partial u/\partial y|$$

WHERE ℓ IS RELATED TO δ, THE CHARACTERISTIC MIXING LAYER THICKNESS

METHODOLOGY IN BOAT

- ON THE AXIS, $\mu_t = \rho \ell^3 \left| \frac{\partial^2 U}{\partial r^2} \right|$
- δ EXTENDS "FULLY" TO EDGE OF MIXING REGION; VARIOUS δ'S ILLUSTRATED ABOVE
- $\ell/\delta = .065$ for $x < x_c$; $\ell/\delta = .08$ for $x > x_c$

Figure 3. Prandtl mixing length model formulation.

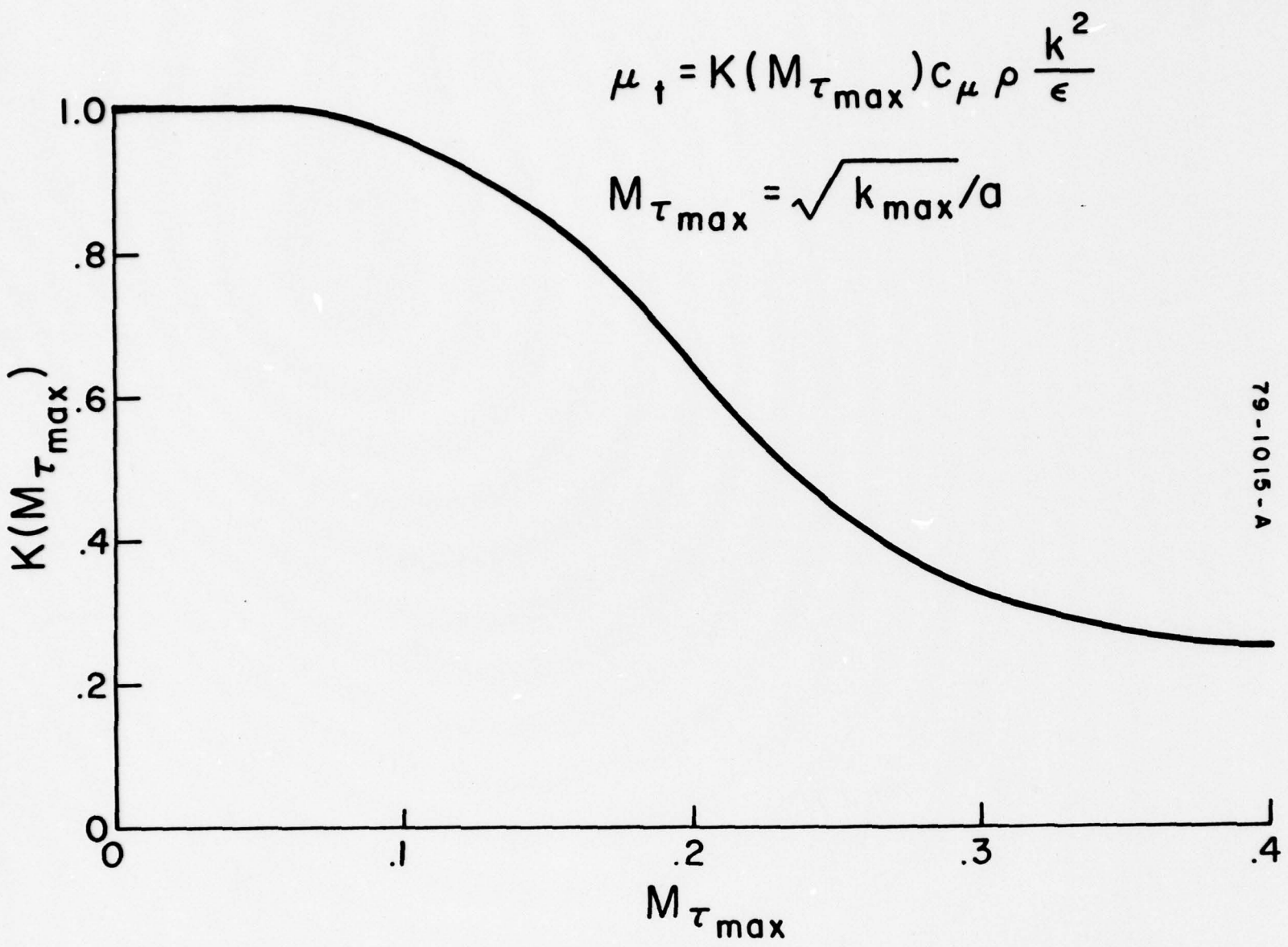

Figure 4. Compressibility correction to basic kε2 model.

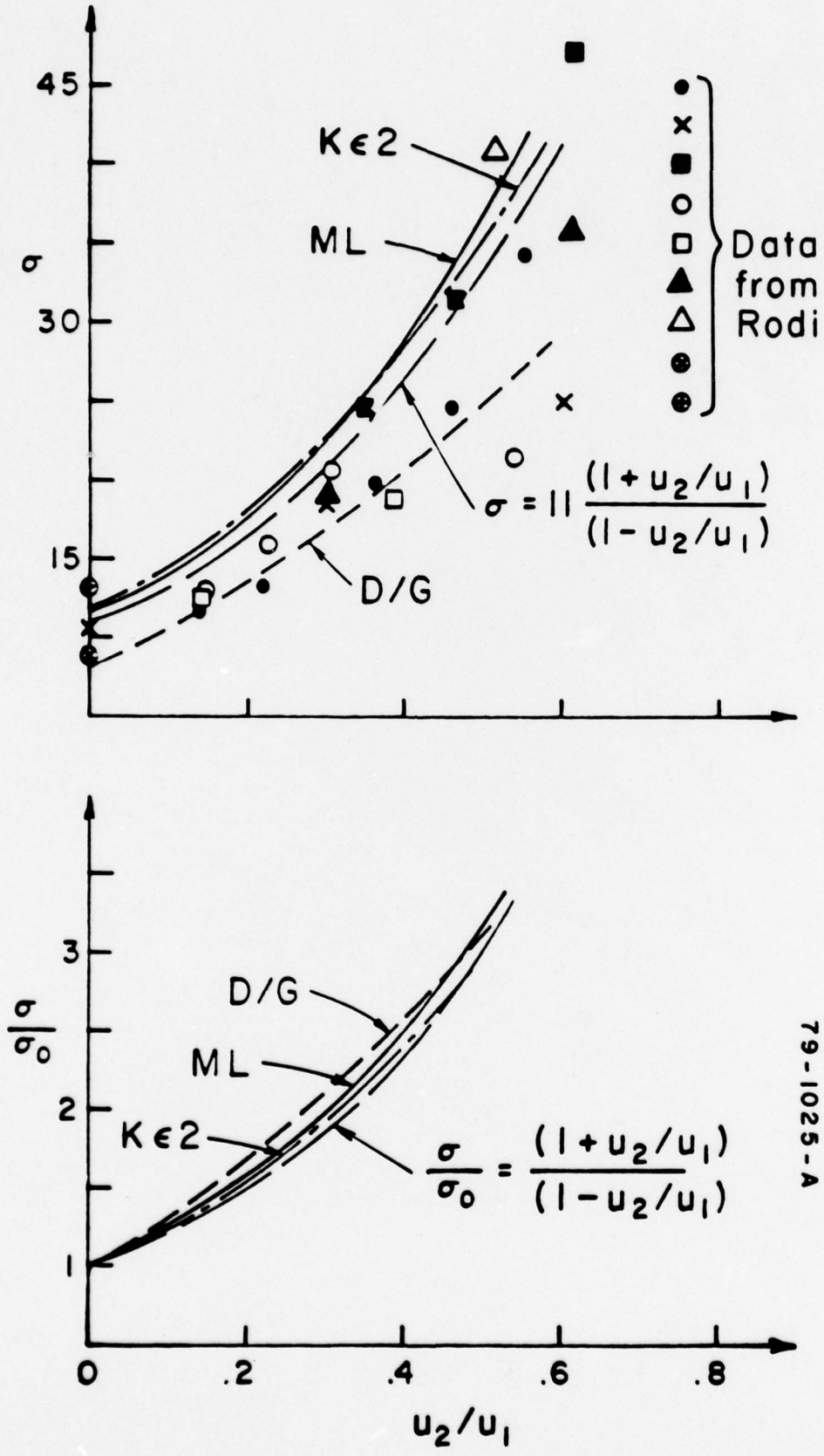

Figure 5. Spread rates for incompressible 2-D shear layers.

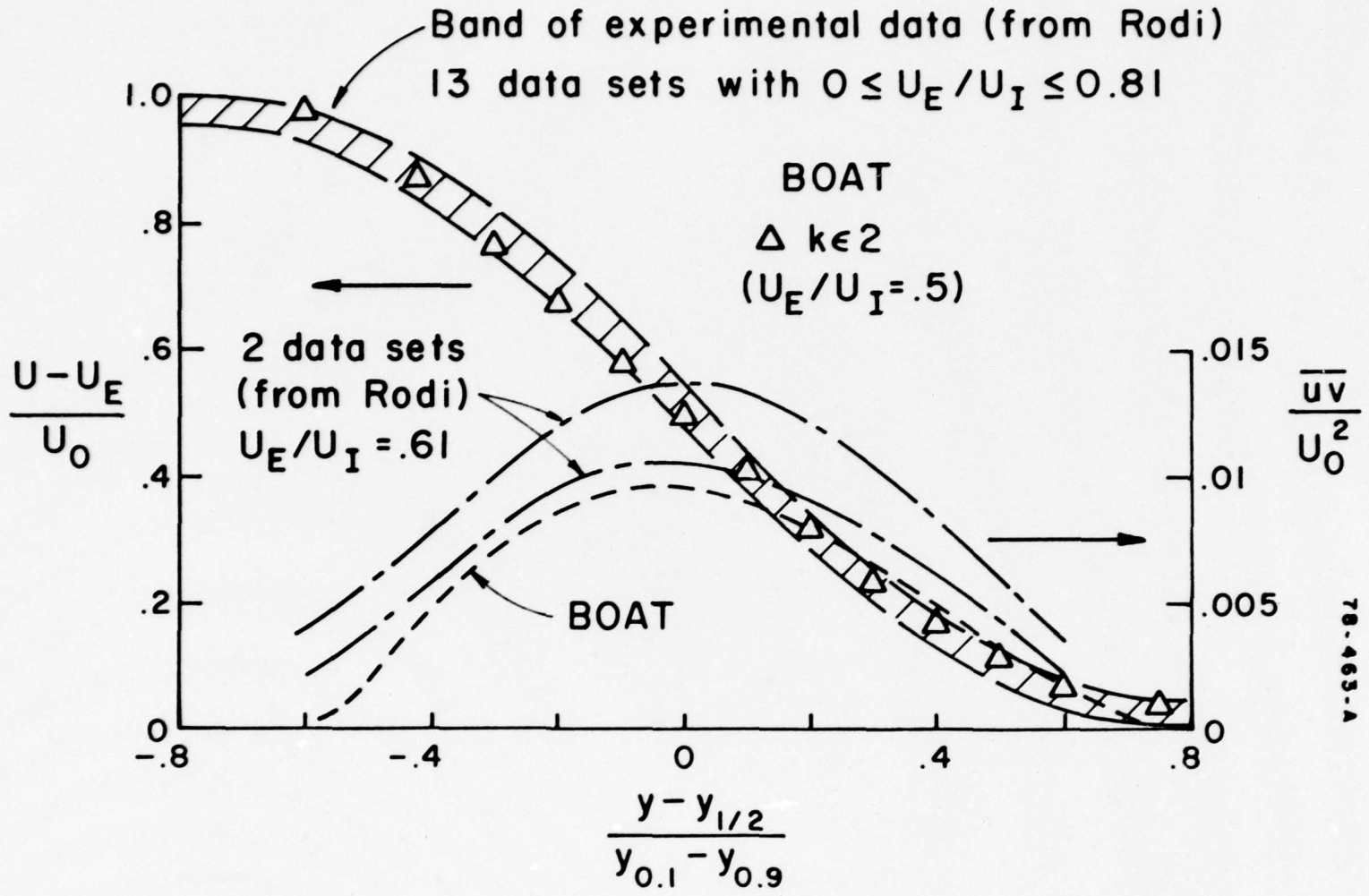

Figure 6. Velocity and shear stress profiles for incompressible 2-D shear layers.

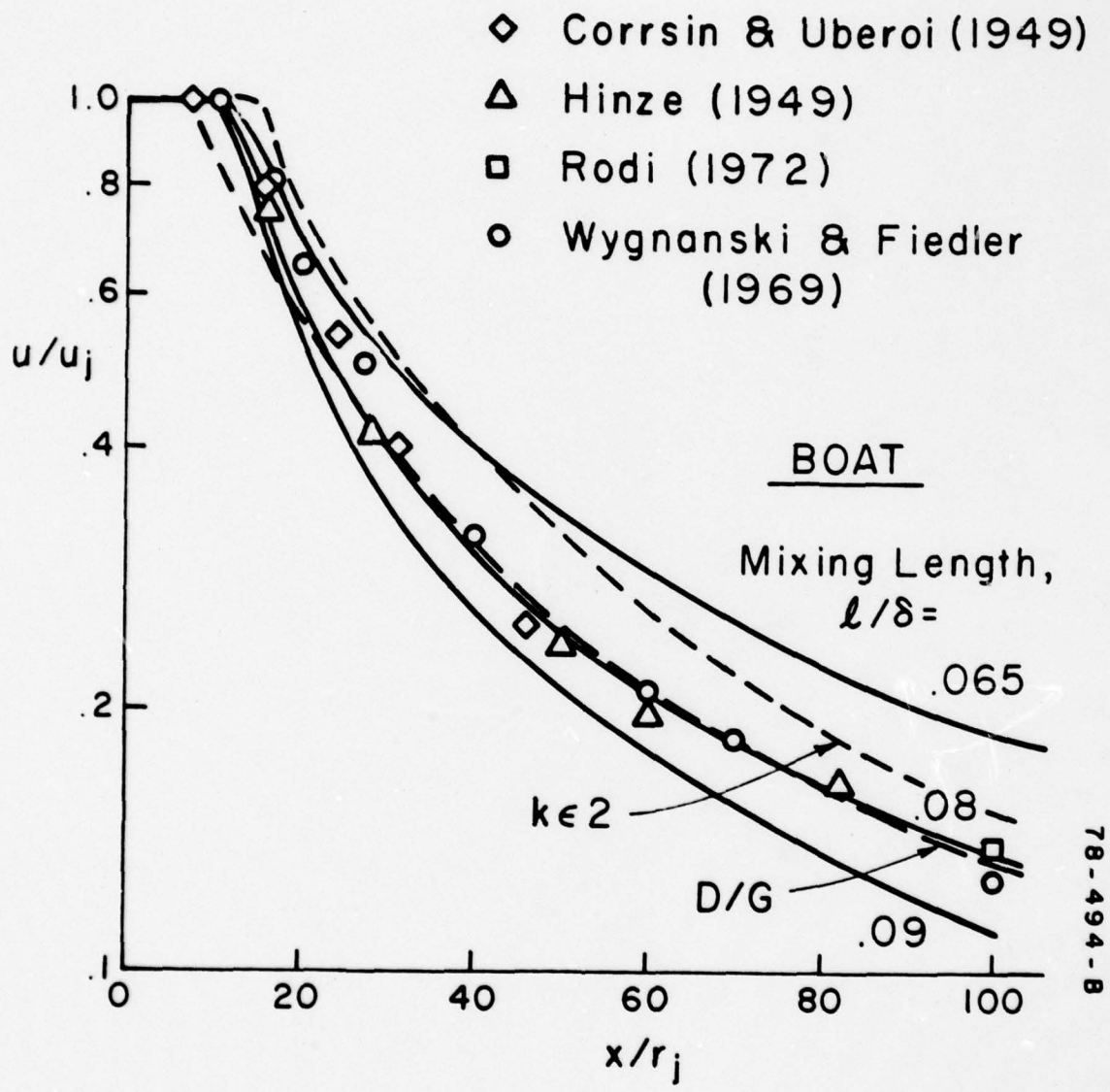

Figure 7. Centerline velocity decay for incompressible jet into still air; initial profiles not specified.

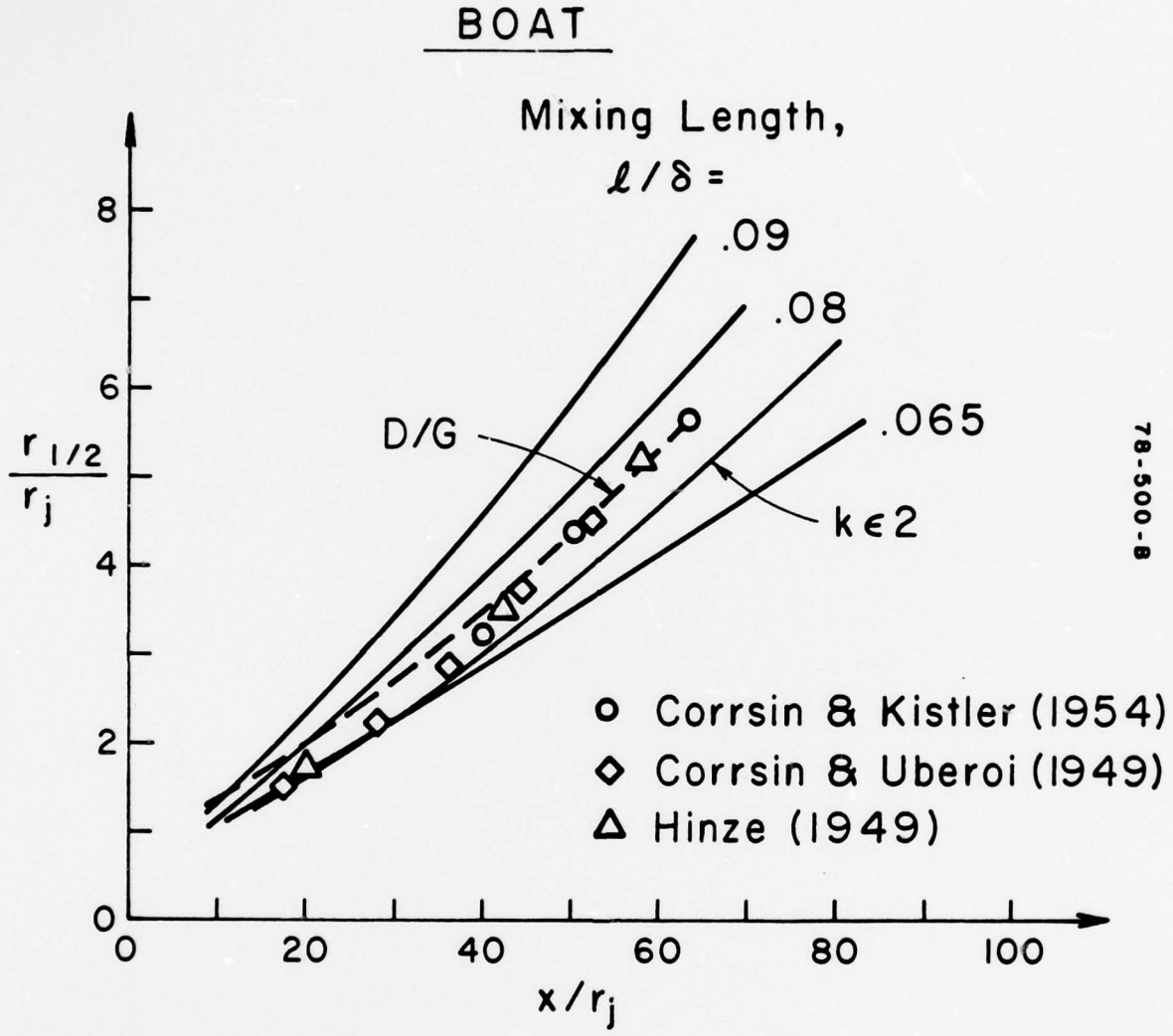

Figure 8. Spread rates for incompressible jet into still air.

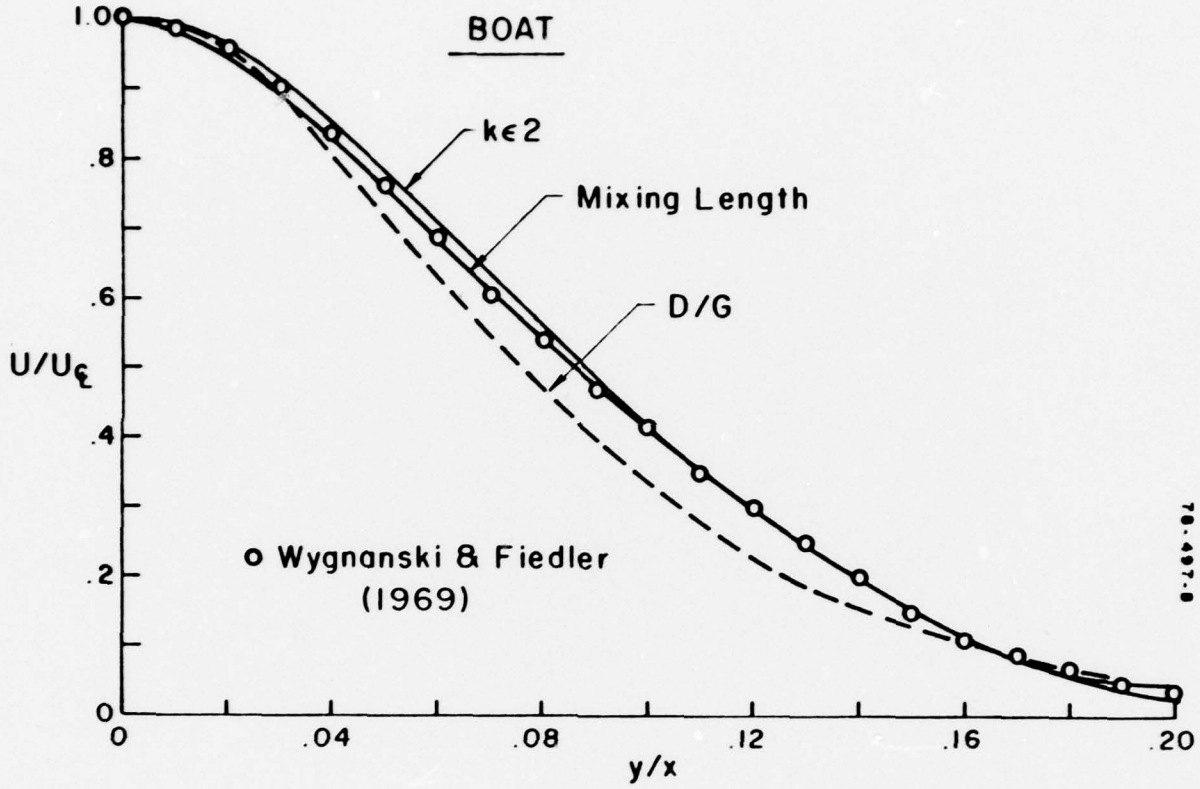

Figure 9. Farfield self-similar velocity profiles; x/r_j = 100; data are from Test Case 18 of Ref. 2.

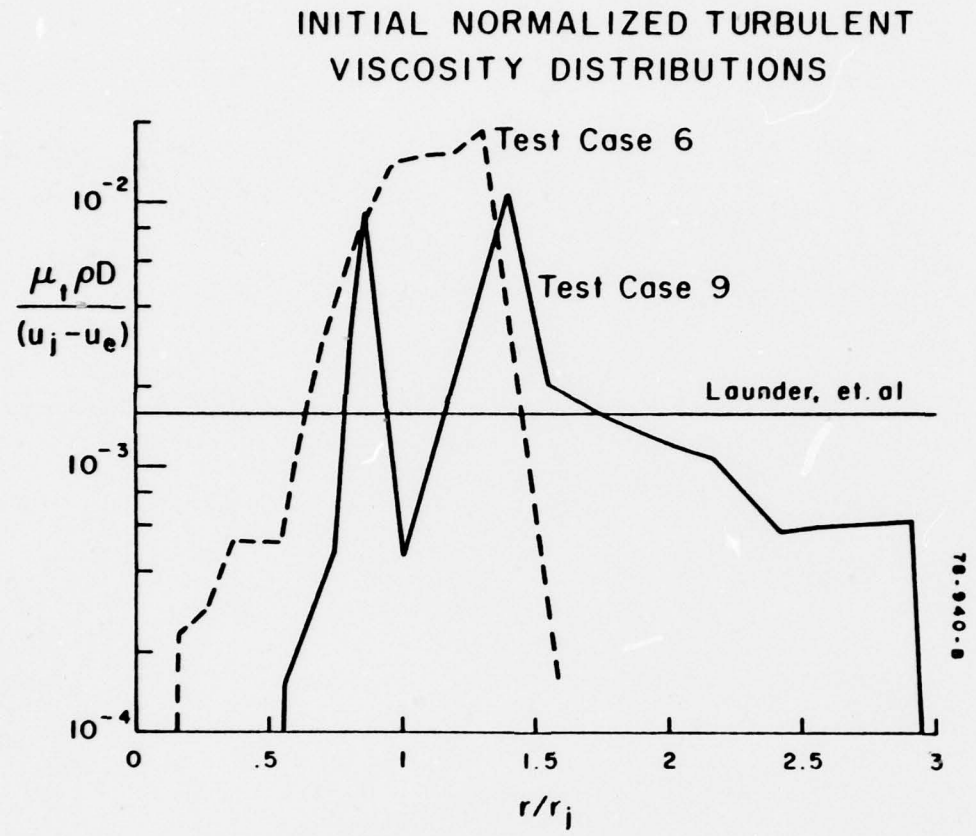

Figure 10. Initial turbulent viscosity for kε2 model calculations; Test Cases 6 and 9 of Ref. 2.

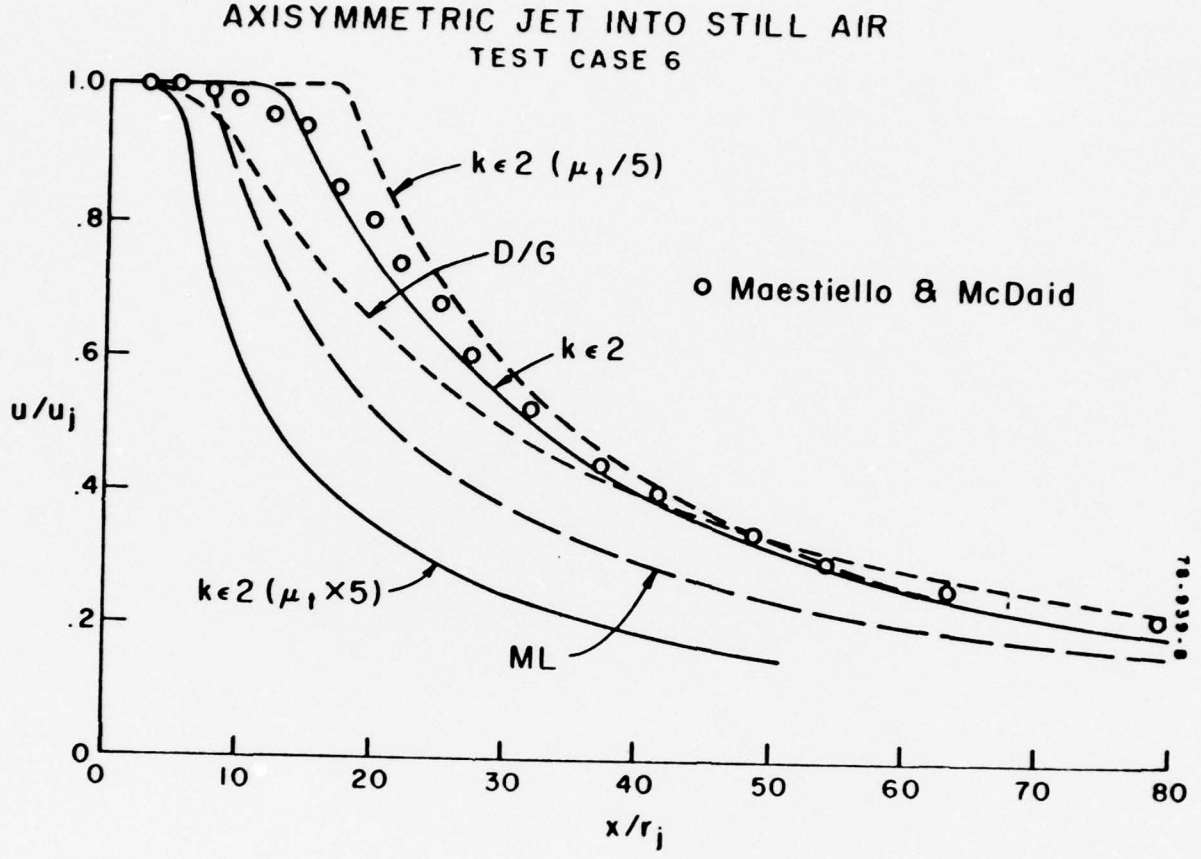

Figure 11. Centerline velocity decay for incompressible jet into still air; influence of initial viscosity on kε2 calculations; Test Case 6 of Ref. 2.

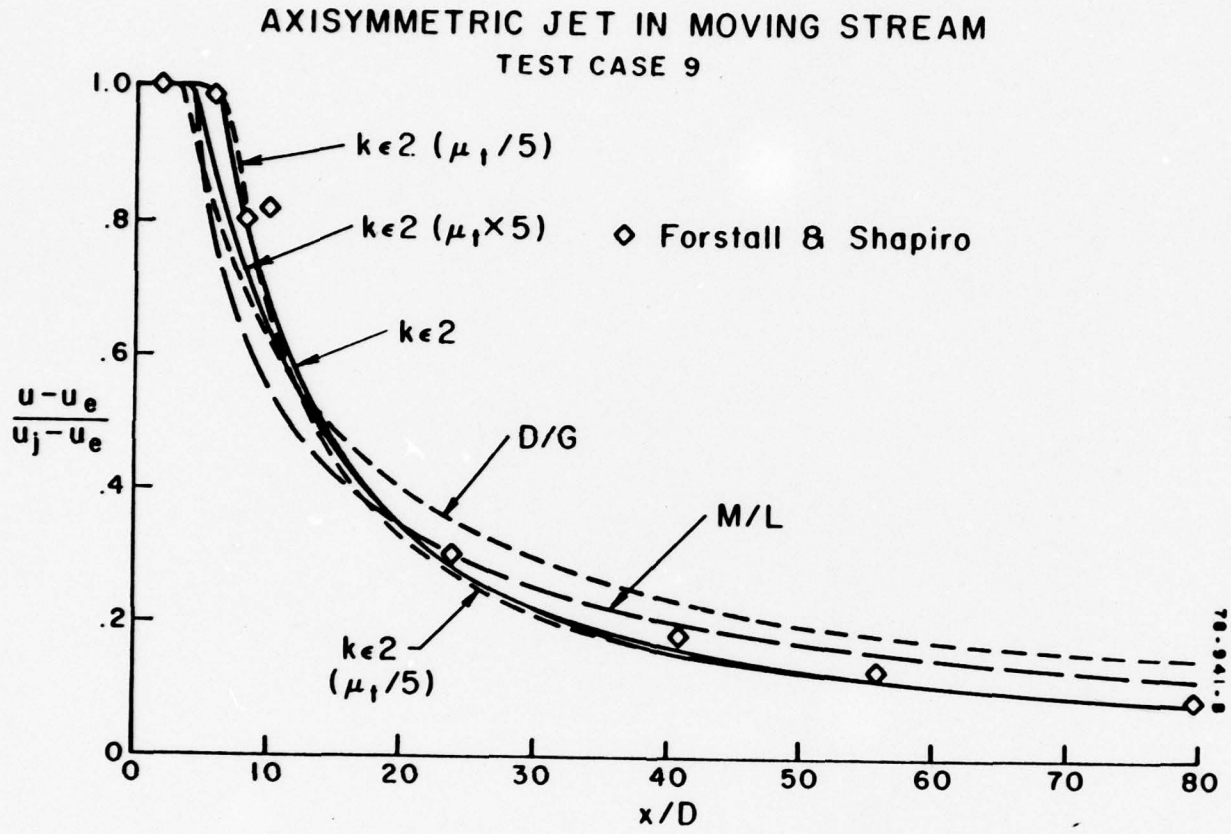

Figure 12. Centerline velocity decay for incompressible jet into moving stream; U_e/U_I = 0.25; influence of initial viscosity on kε2 calculations; Test Case 9 of Ref. 2.

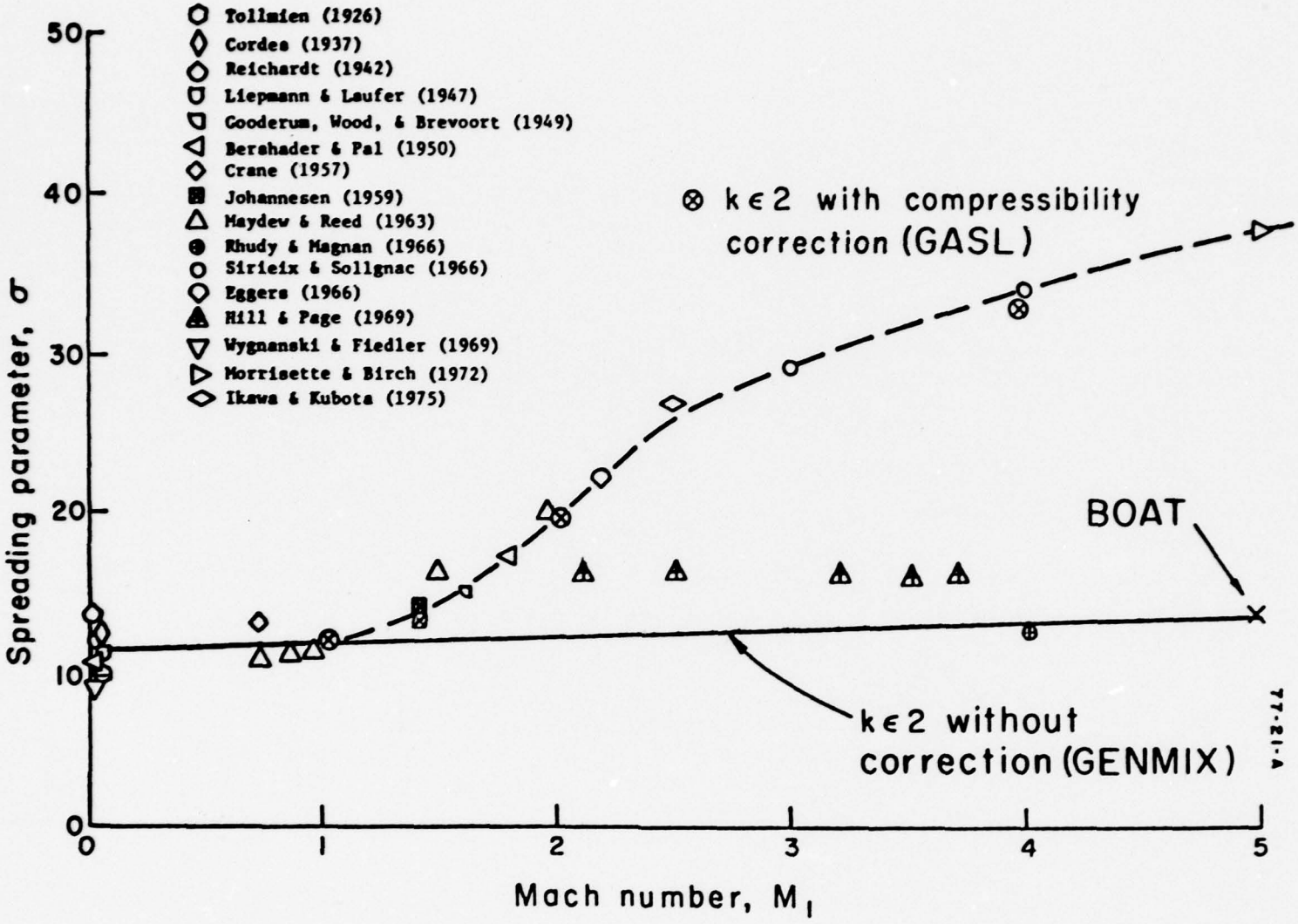

Figure 13. Spread rates for isoenergetic compressible 2-D shear layers; data from Ref. 2.

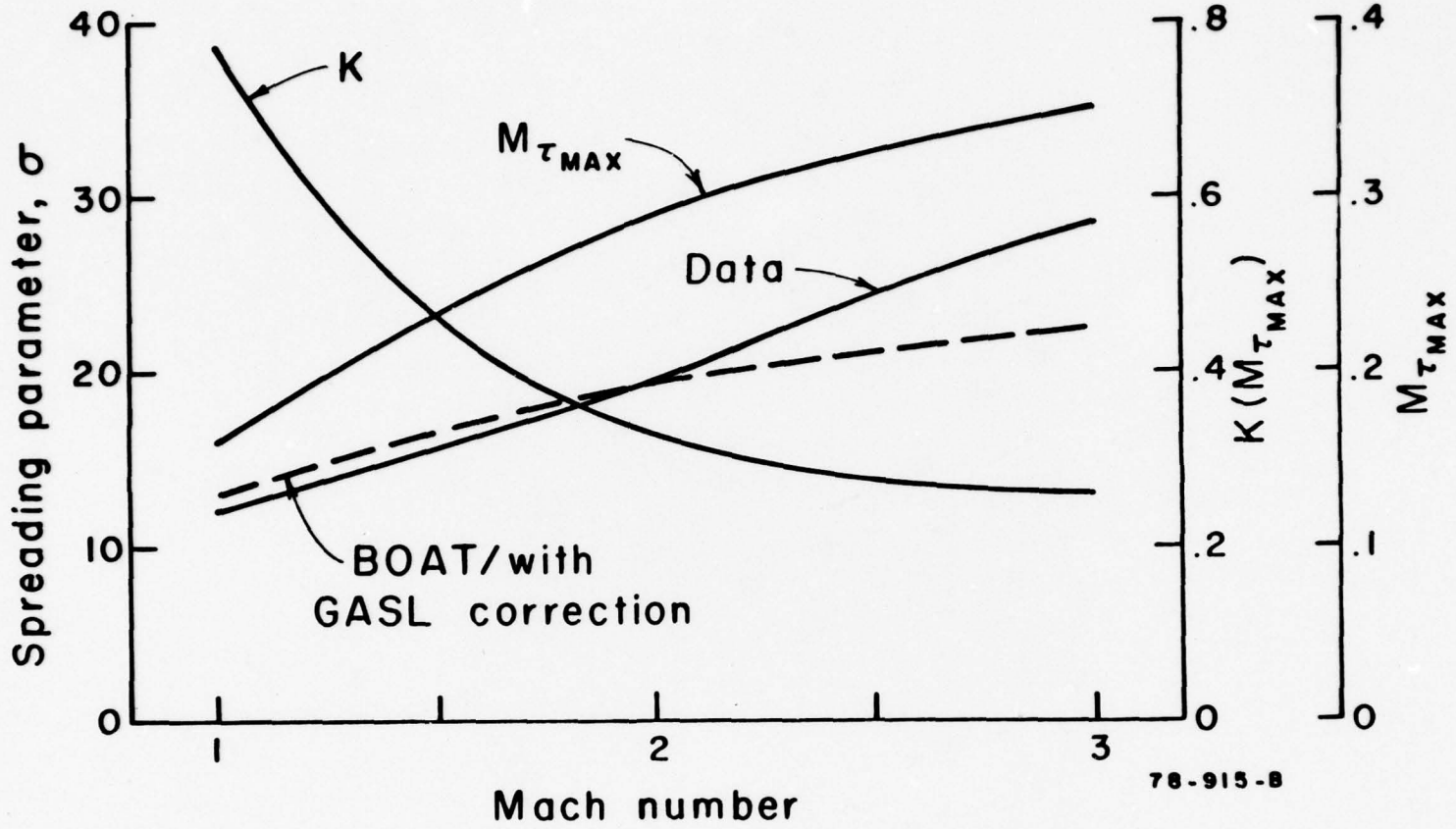

Figure 14. Comparison between spread rate data on compressible 2-D shear layers and BOAT calculations with compressibility corrected kε2 model.

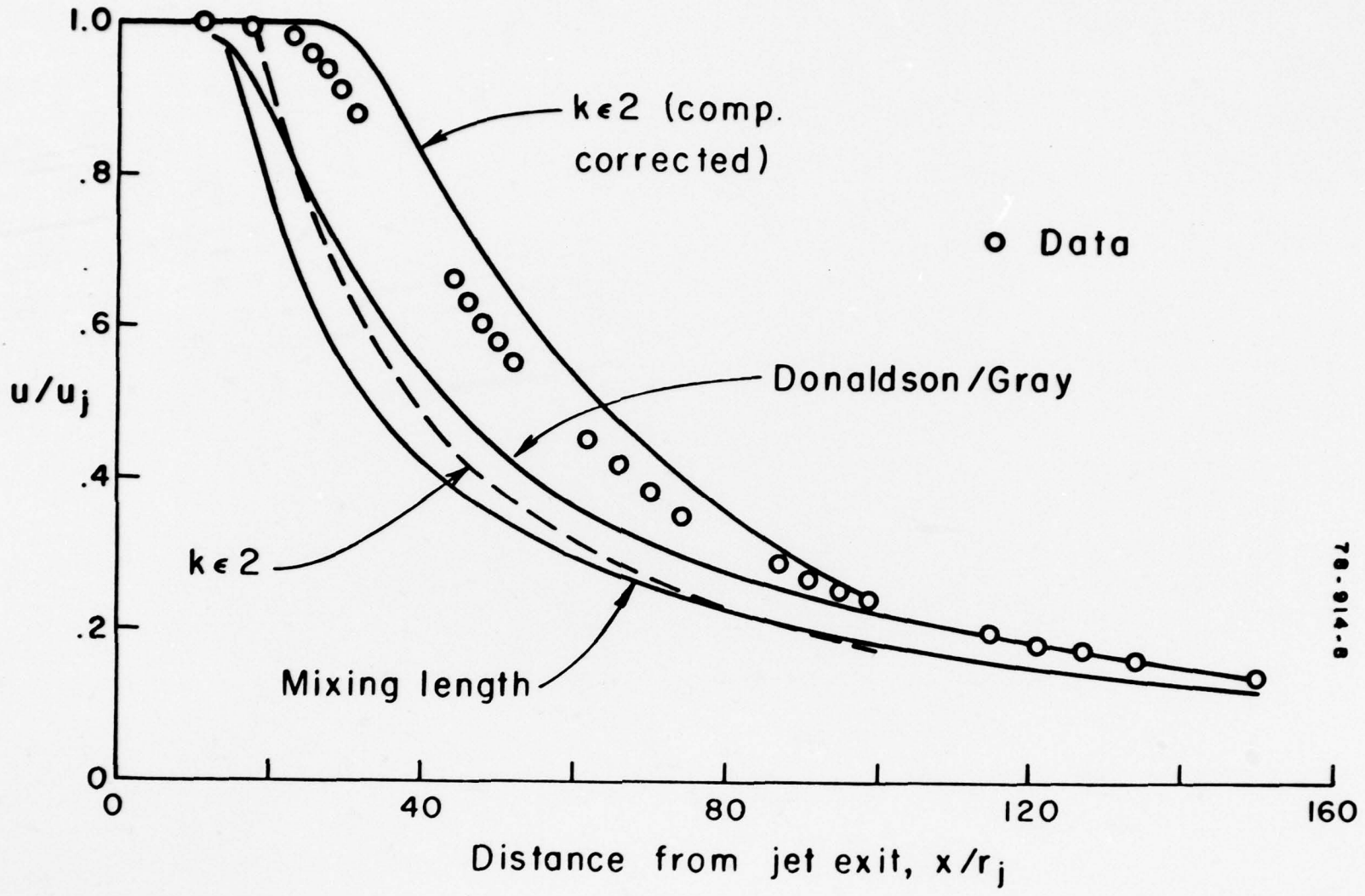

Figure 15. Centerline velocity decay for Mach 2.2 air jet into still air; Test Case 7 of Ref. 2.

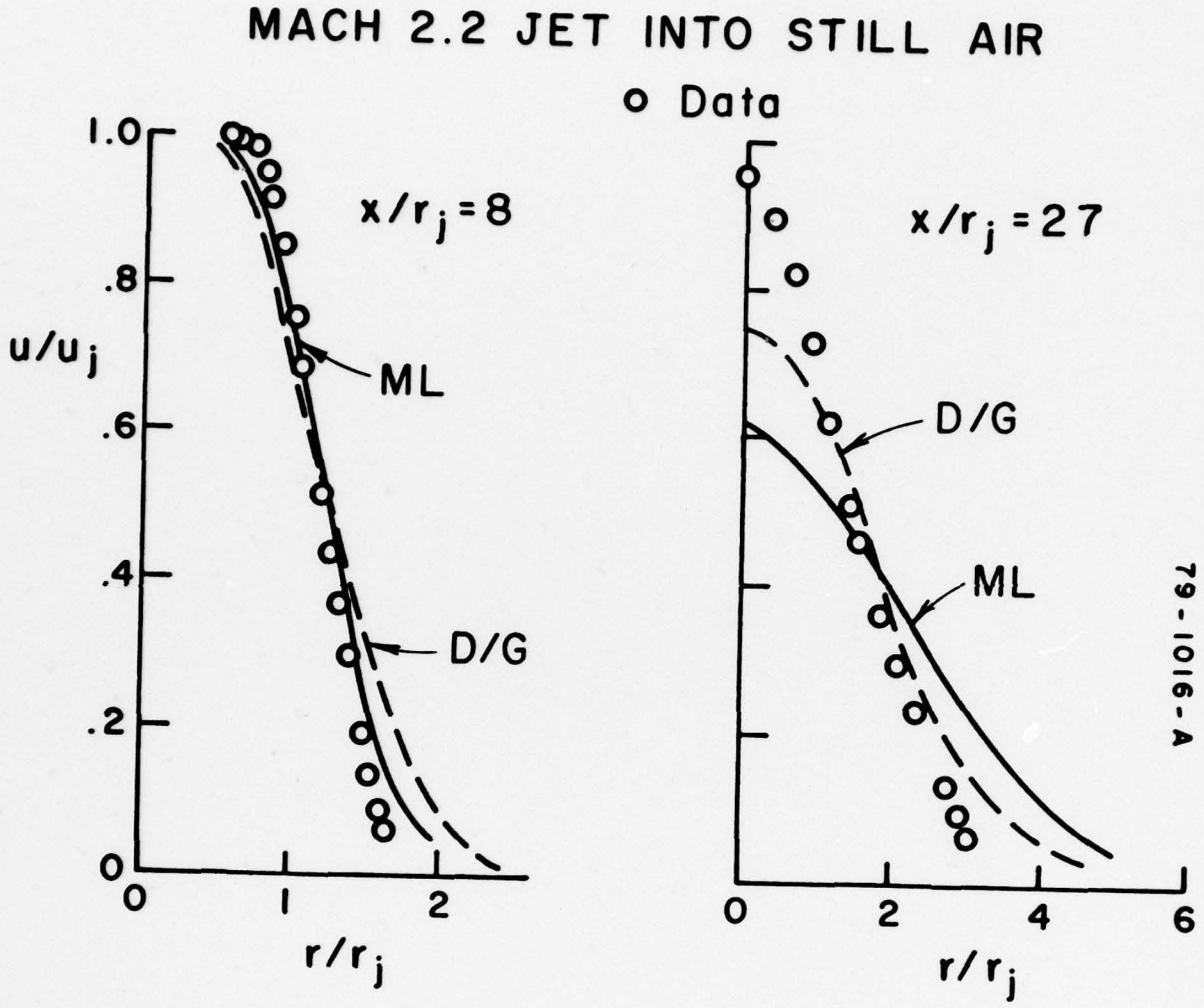

Figure 16a. Radial velocity profiles for Mach 2.2 air jet into still air; x/r_j = 8 and 27.

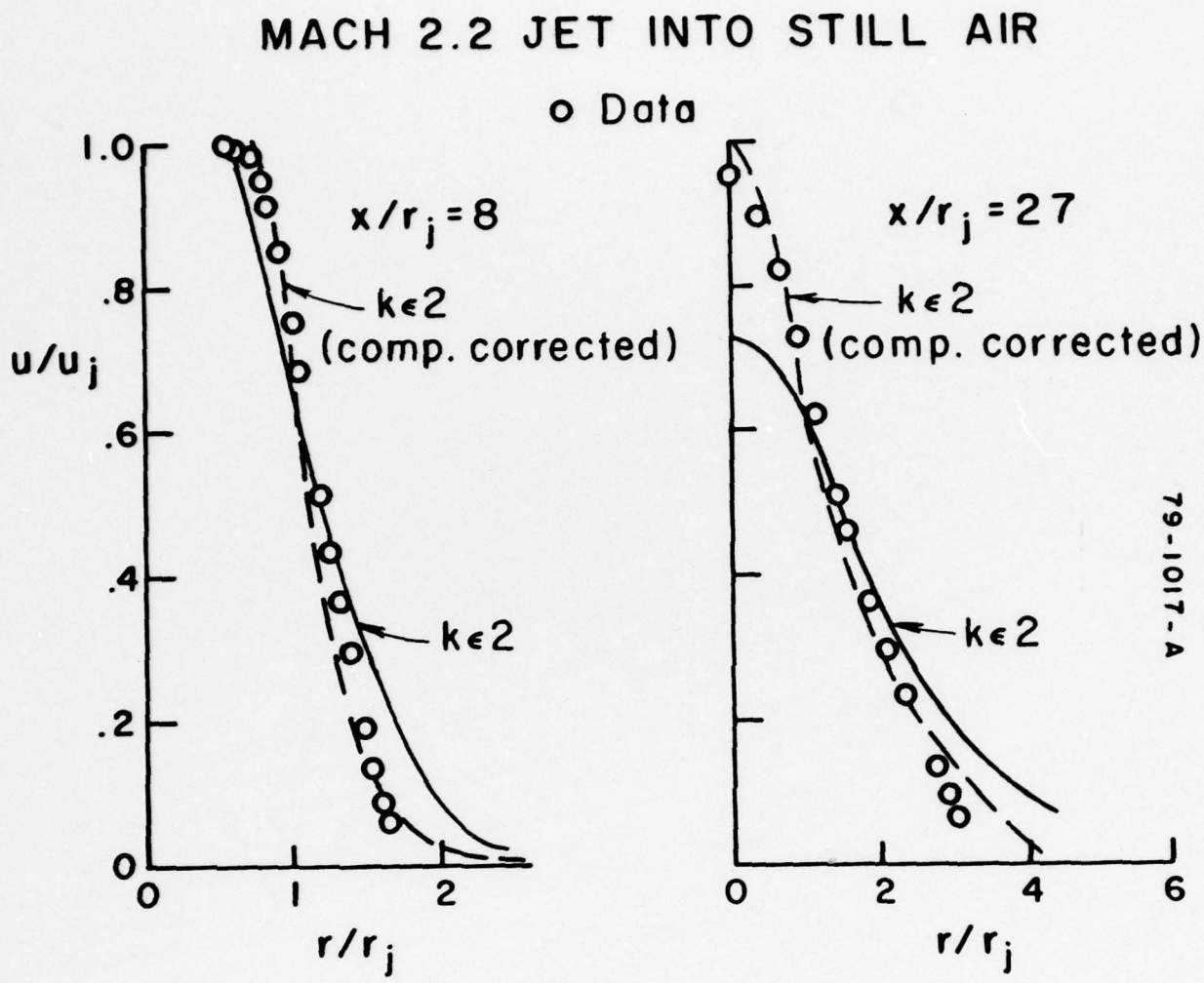

Figure 16b. Radial velocity profiles for Mach 2.2 air jet into still air; x/r_j = 8 and 27.

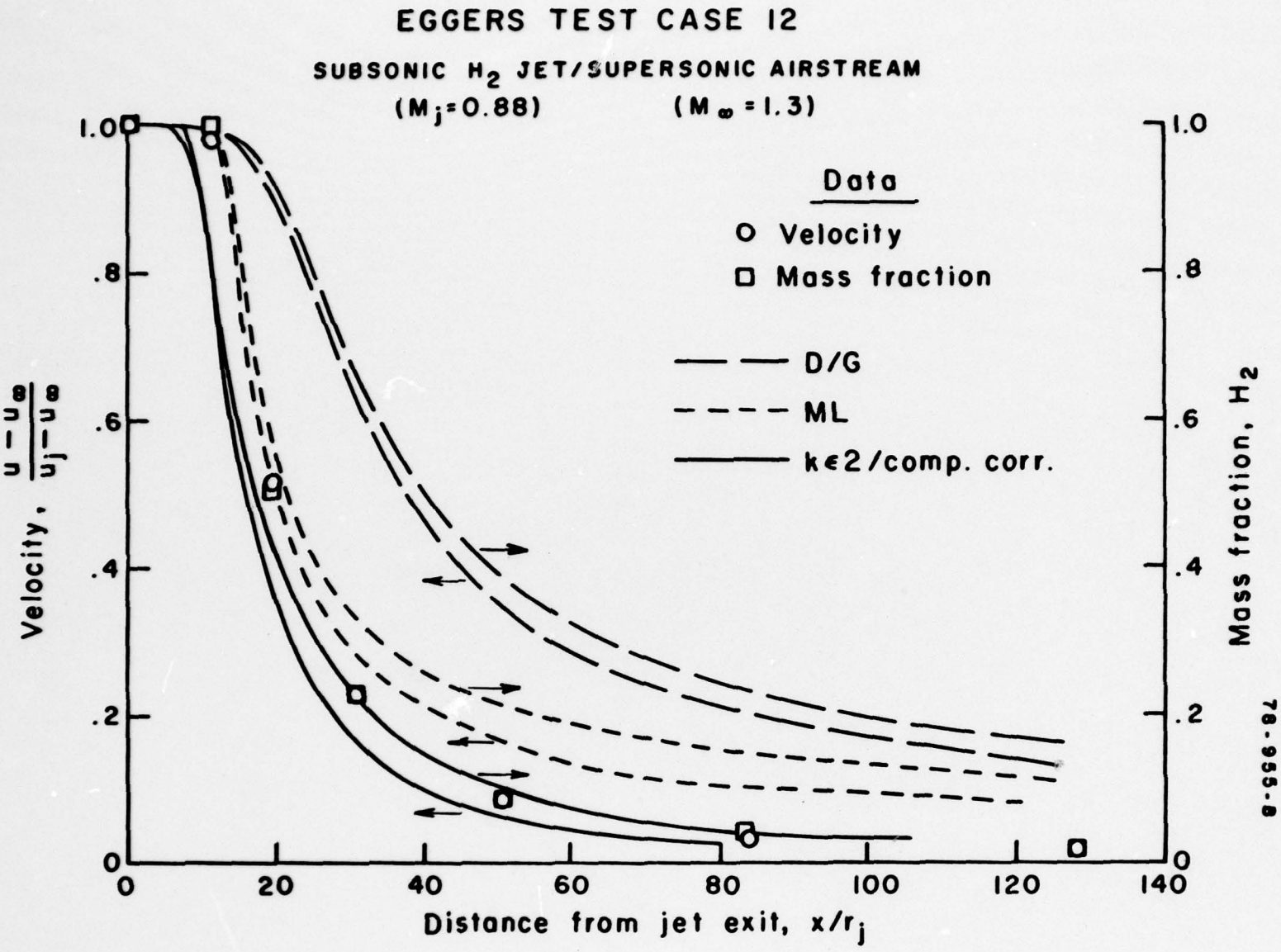

Figure 17. Centerline velocity and H_2 mass fraction decay for subsonic H_2 jet into supersonic airstream.

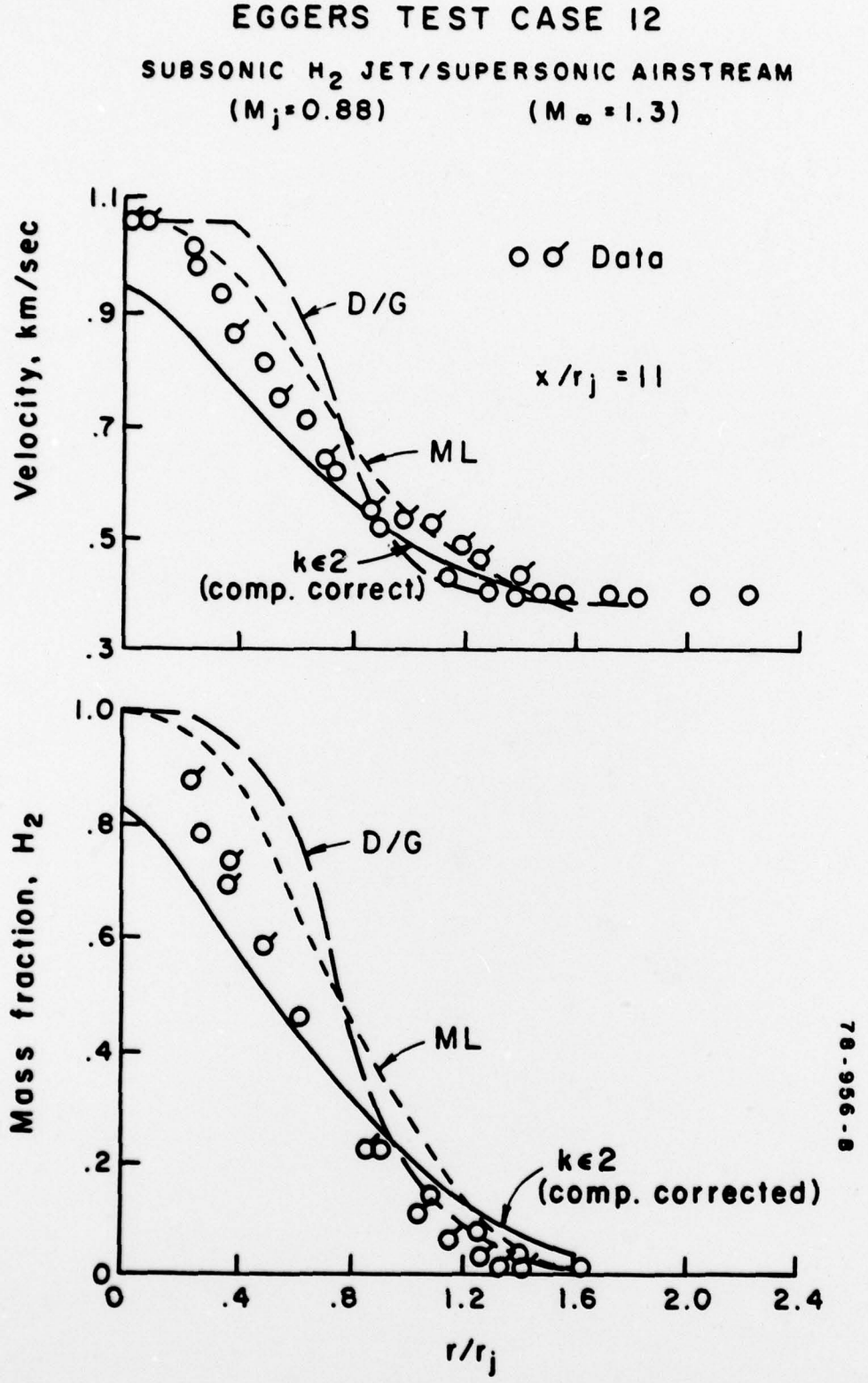

Figure 18a. Radial velocity and H_2 mass fraction profiles for subsonic H_2 jet into supersonic airstream; x/r_j = 11.

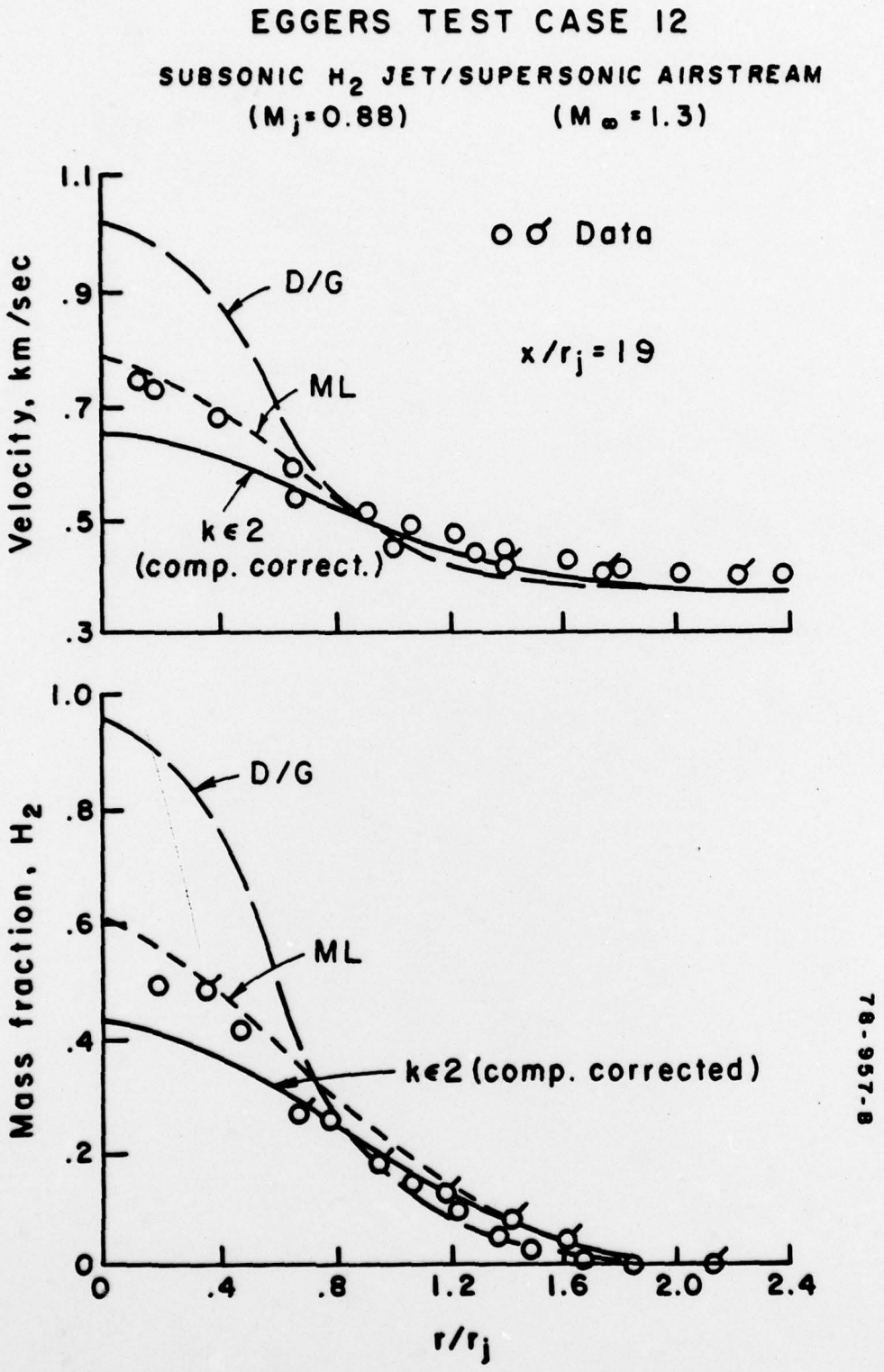

Figure 18b. Radial velocity and H_2 mass fraction profiles for subsonic H_2 jet into supersonic airstream; x/r_j = 19.

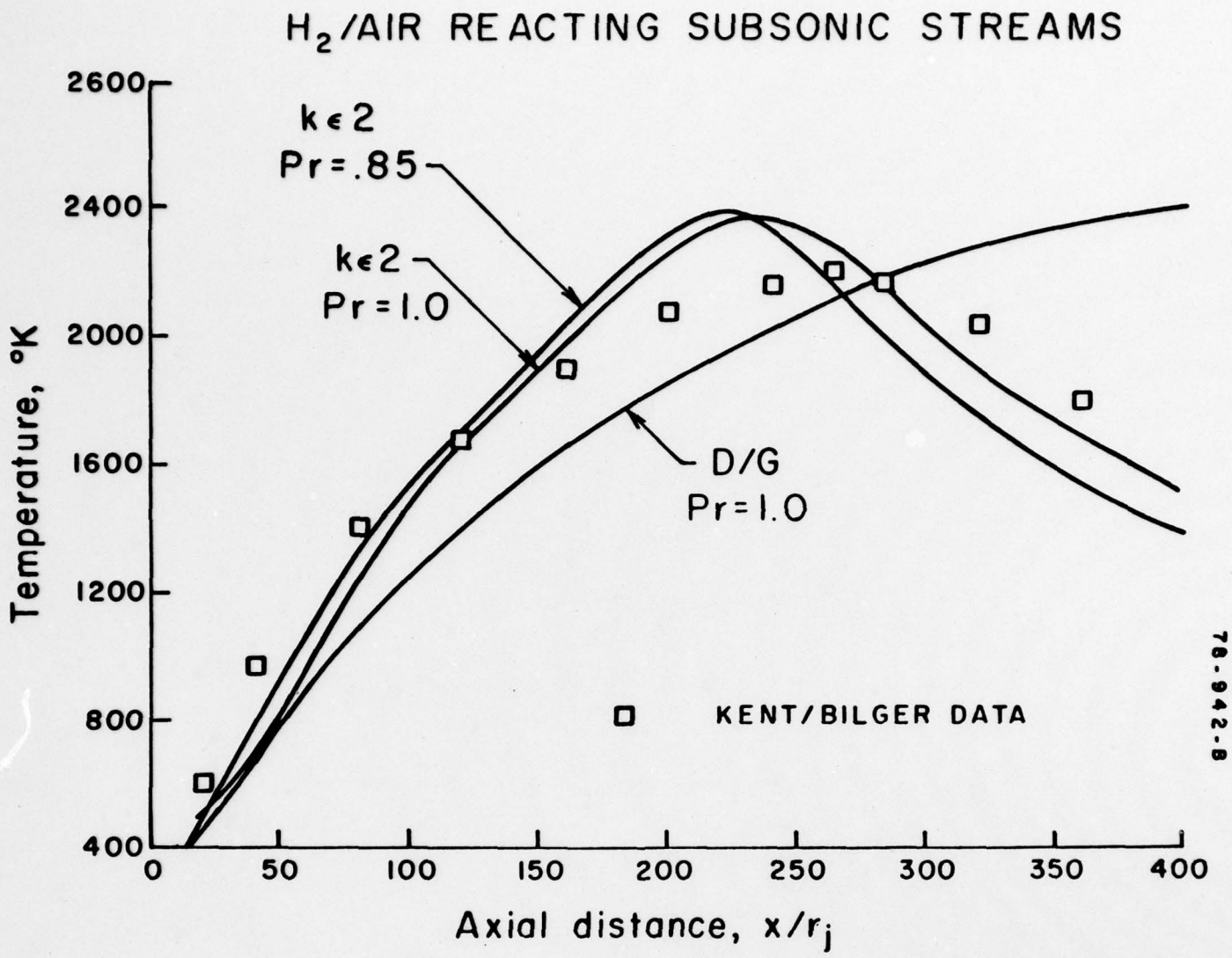

Figure 19. Centerline temperature profiles for H_2/air reacting subsonic streams.

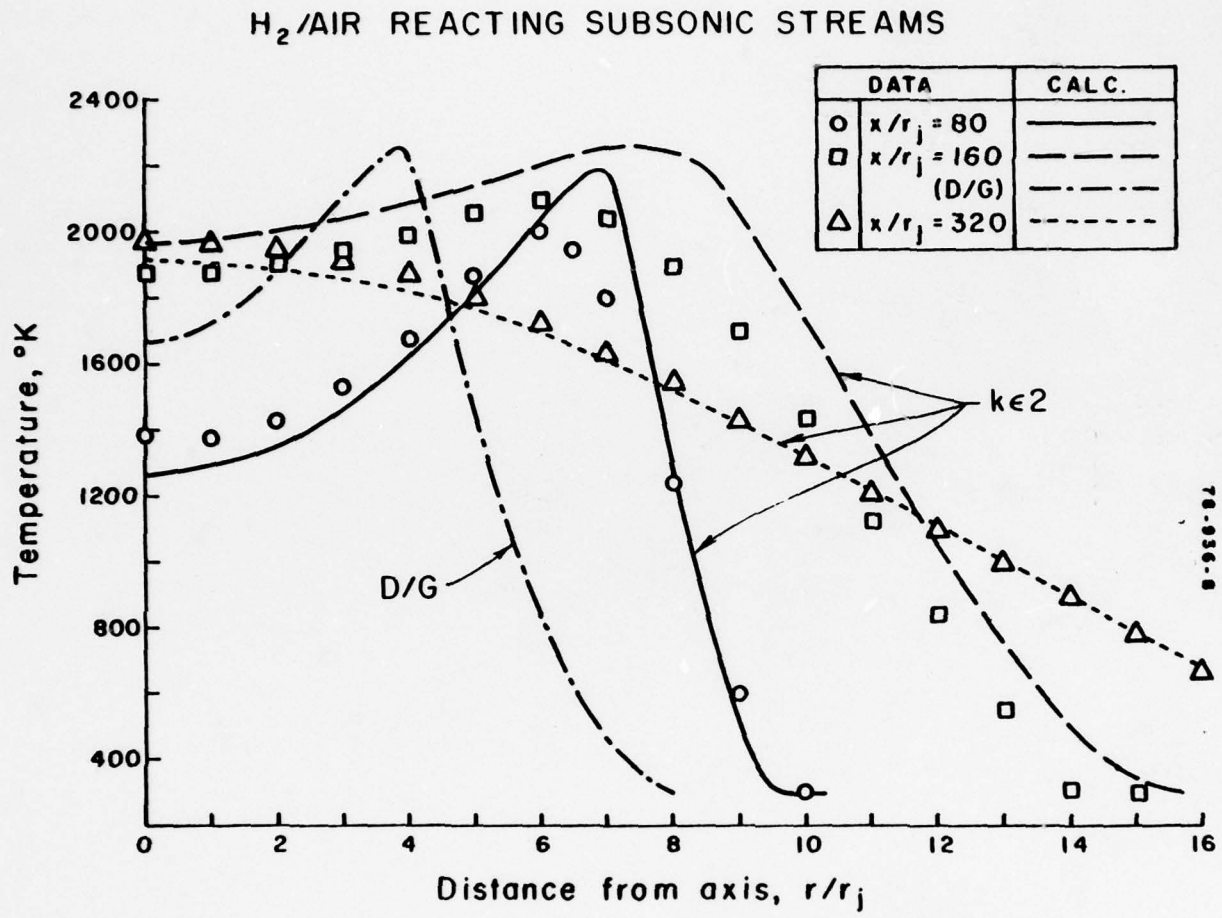

Figure 20. Radial temperature profiles for the H_2/air reacting subsonic streams.

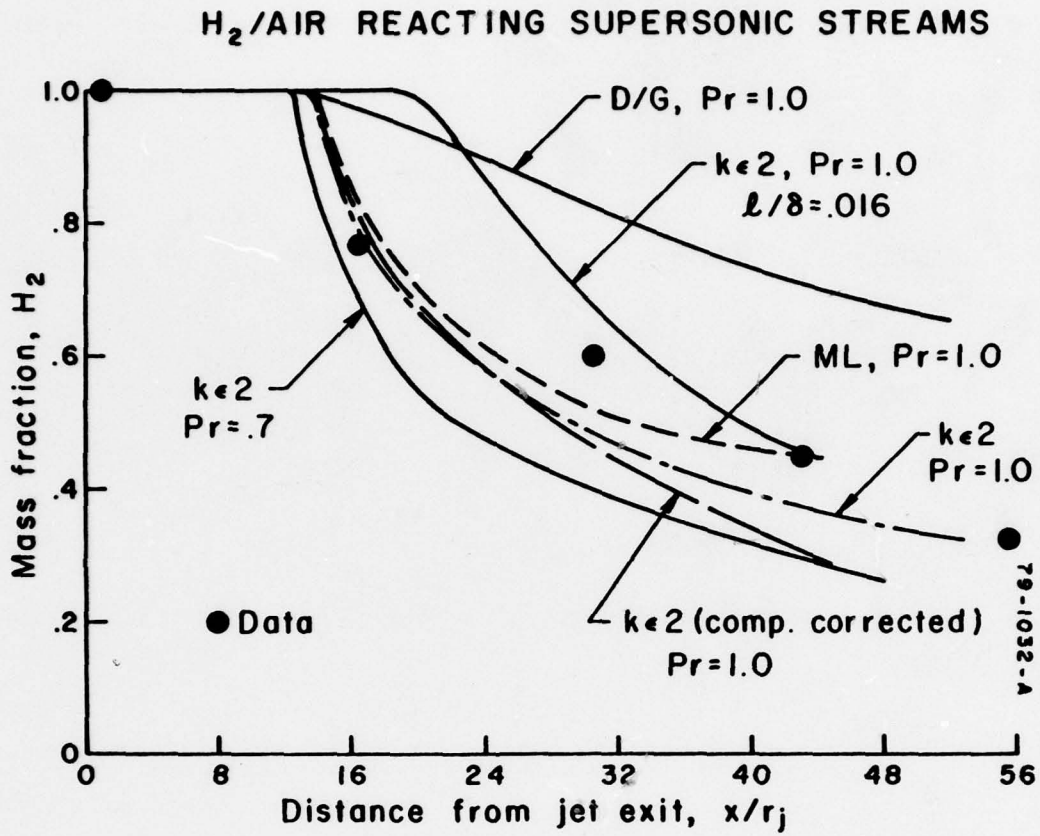

Figure 21. Centerline H_2 mass fraction profiles in H_2/air reacting supersonic streams.

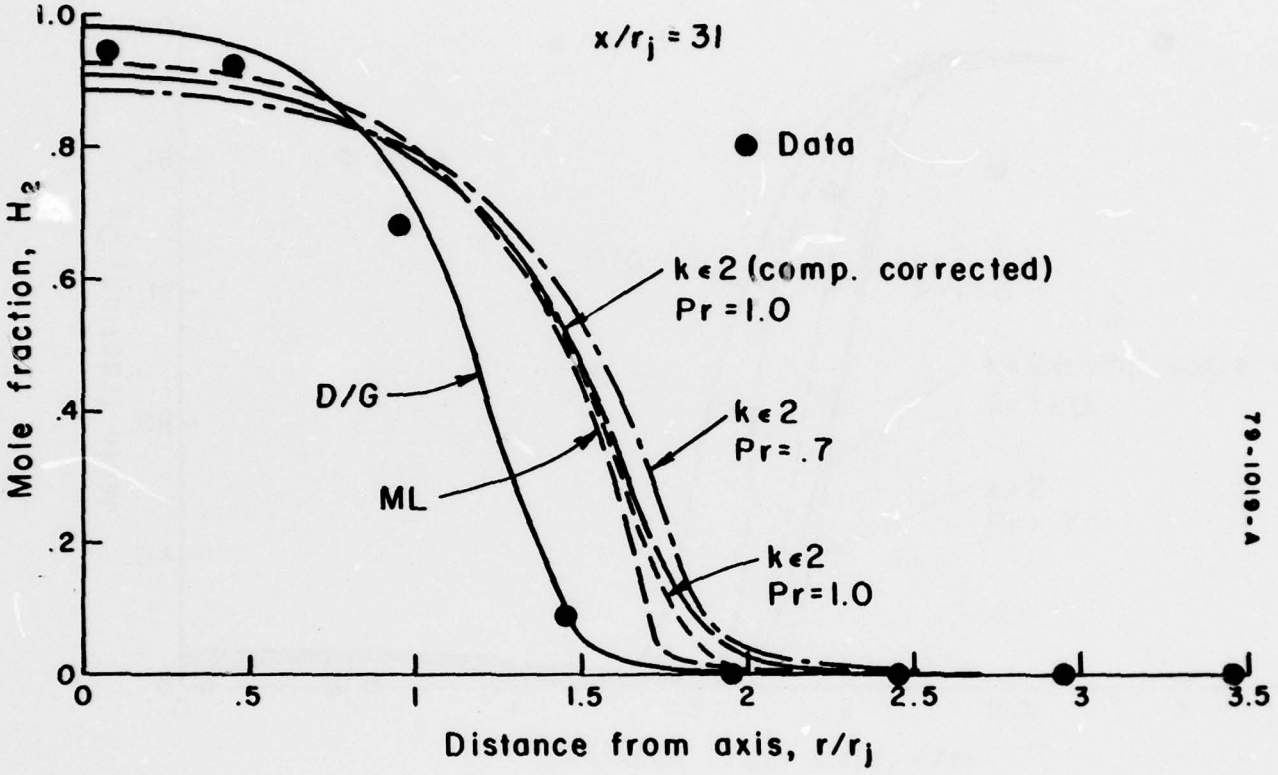

Figure 22a. Radial H_2 mole fraction profiles for H_2/air reacting supersonic streams.

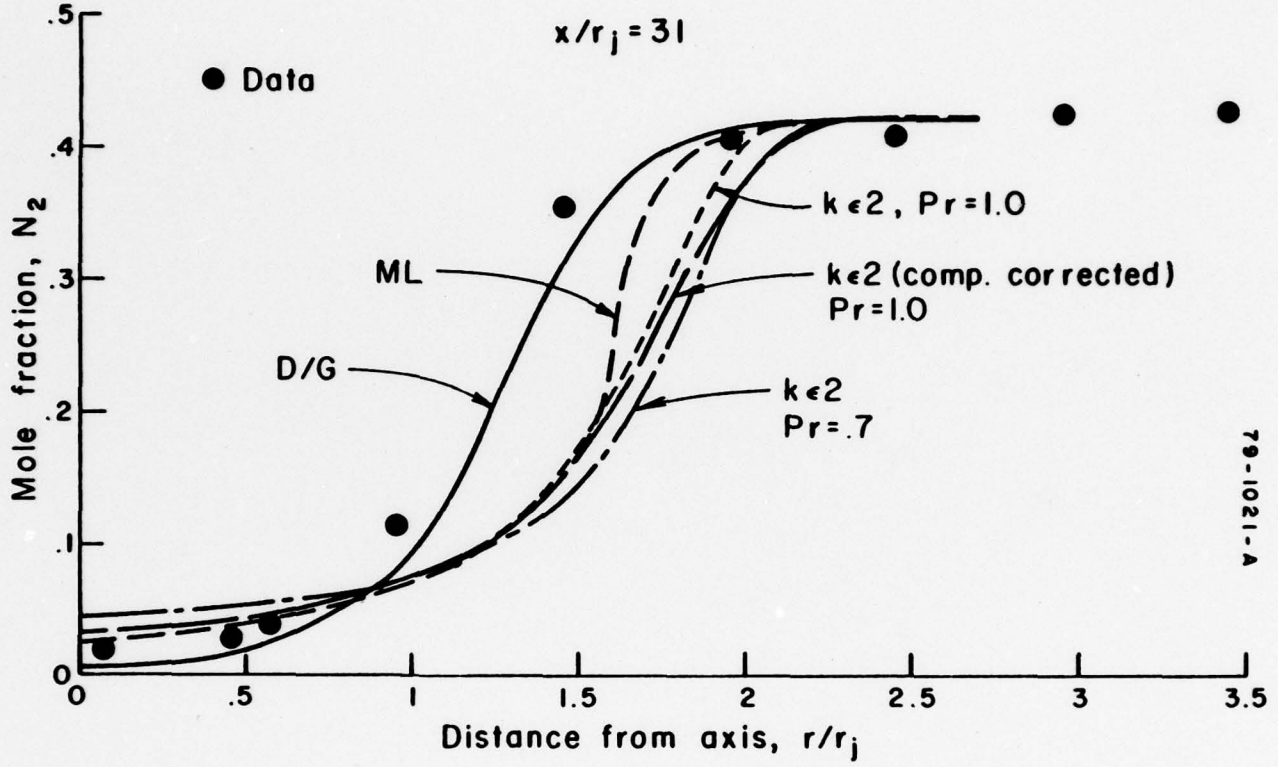

Figure 22c. Radial N_2 mole fraction profiles for H_2/air reacting supersonic streams.

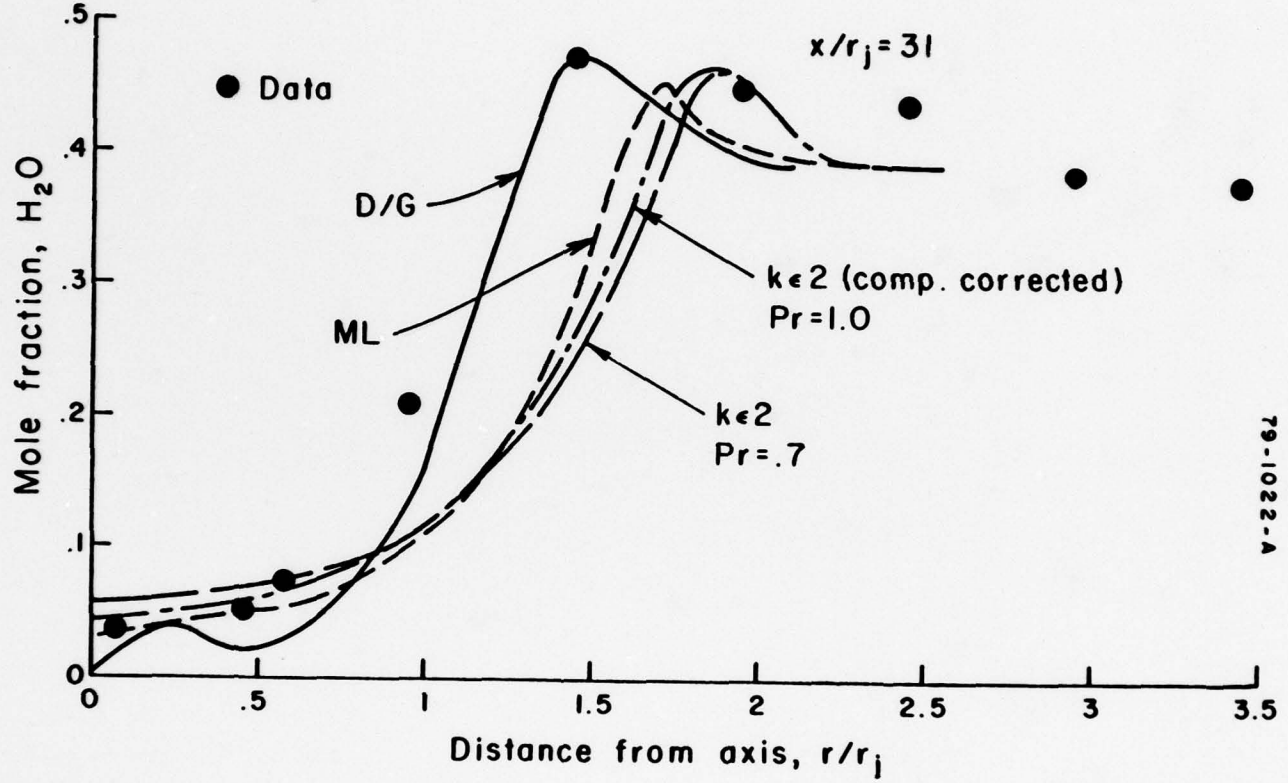

Figure 22d. Radial H_2O mole fraction profiles for H_2/air reacting supersonic streams.

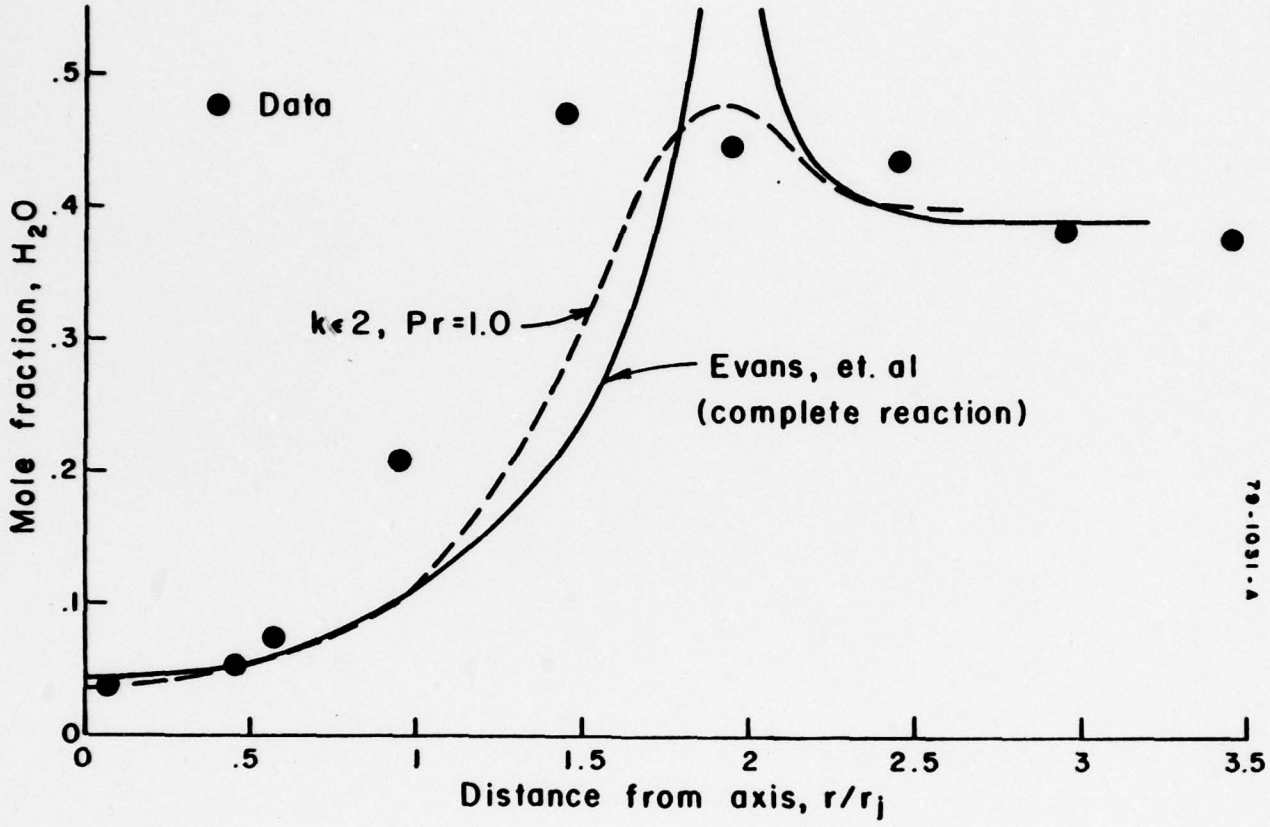

Figure 22e. Radial H_2O mole fraction profiles for H_2/air reacting supersonic streams.

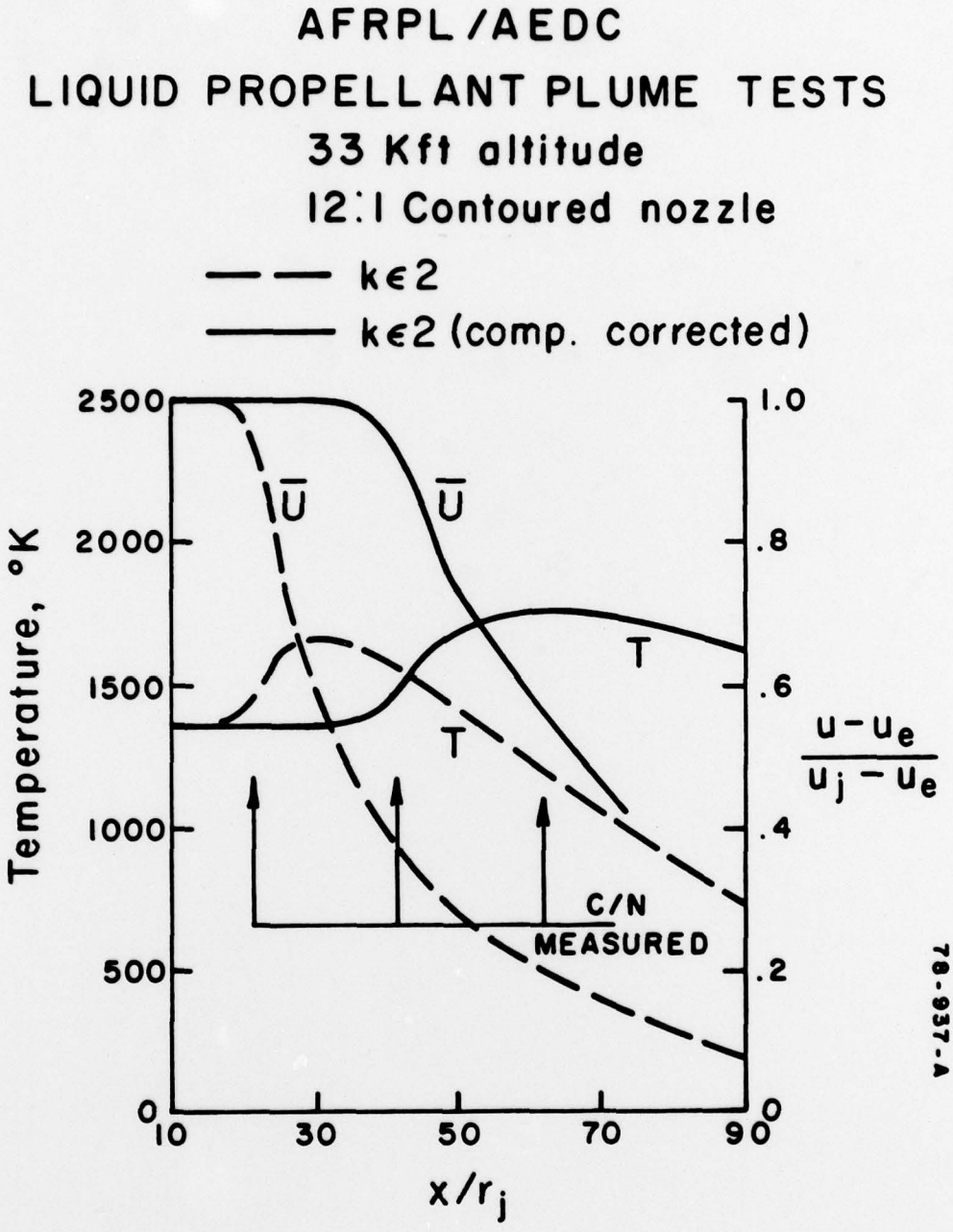

Figure 23. Predicted centerline temperature and velocity profiles for liquid propellant plume test.

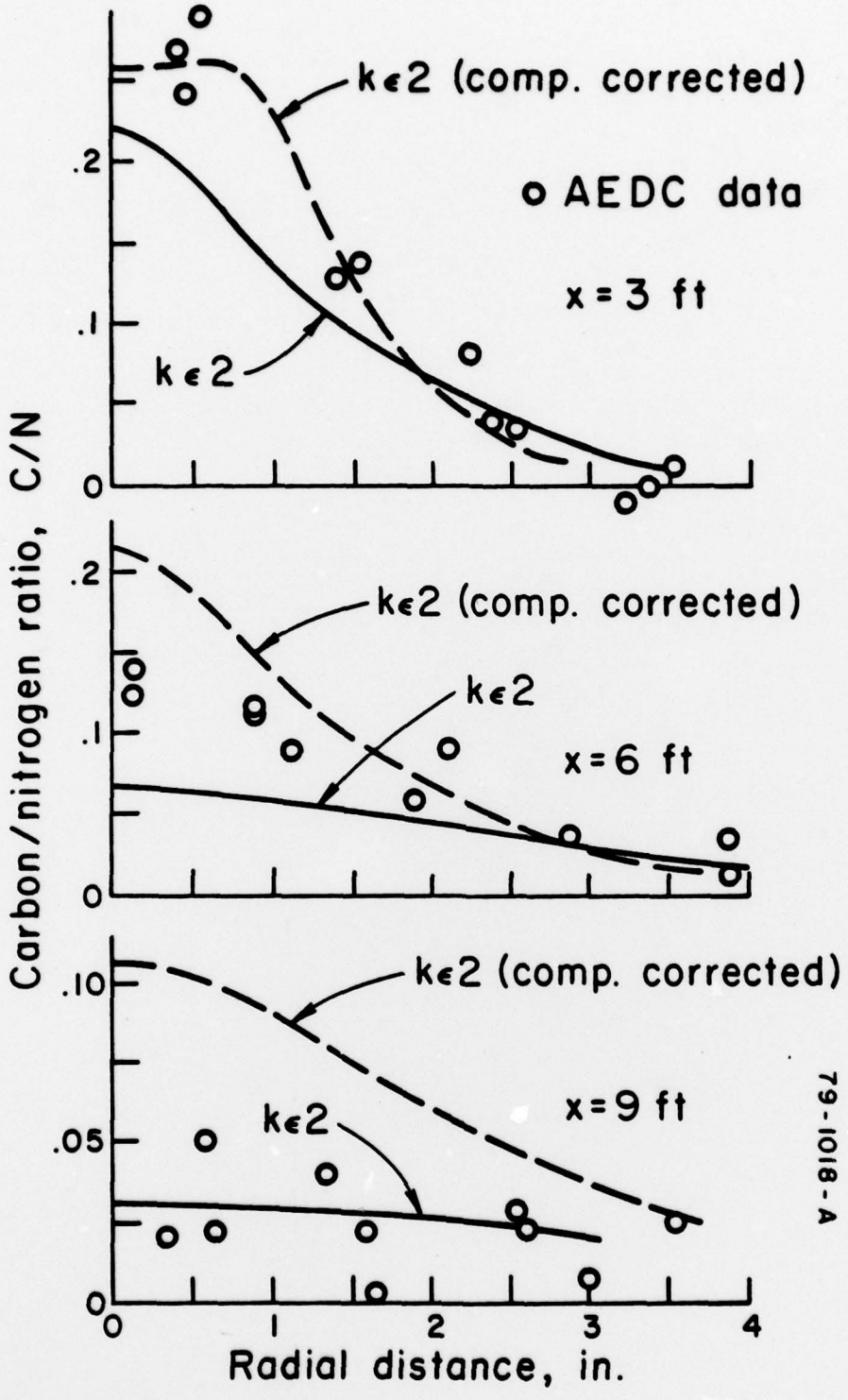

Figure 24. Measured and predicted carbon/nitrogen ratios for liquid propellant plume test.